AN AUTOMATED ANALYSIS
OF SECONDARY ISOTOPE EFFECTS
IN
AQUEOUS ALKALINE ESTER HYDROLYSIS

Thesis for the Degree of Ph. D.
MICHIGAN STATE UNIVERSITY
WILLIAM CHARLES SASS
1970

This is to certify that the

thesis entitled

An Automated Analysis of Secondary Isotope
Effects in Aqueous Alkaline Ester Hydrolysis

presented by

William Charles Sass

has been accepted towards fulfillment
of the requirements for

Ph.D. degree in Chemistry

G. J. Karabatsos
Major professor

Date Aug. 24, 1970

O-169

ABSTRACT

An Automated Analysis of Secondary Isotope Effects In Aqueous Alkaline Ester Hydrolysis

By

William Charles Sass

The β-secondary kinetic isotope effect observed in the aqueous alkaline hydrolysis of ethyl acetate-$\underline{d}_3$ at 25° has been reported by Bender and Feng (1). Incorporation of this value into the results of a temperature study of the kinetic isotope effect conducted by Halevi and Margolin (2) revealed an unprecedented temperature dependence of the isotope effect. The values reported are:

Temp	0°	25°	35°	65°
k_H/k_D	1.00±0.01	0.90±0.01	0.93±0.01	1.15±0.09

Both kinetic studies were based on titration techniques.

In this study the design of a family of automated instruments capable of a continuously following ester hydrolysis and other reactions in which acid or base is generated is discussed. Two of the instruments were built and found to perform well. The speed and accuracy of one of the instruments made it ideally suited to verify the important temperature dependence reported by Halevi. Temperature studies on ethyl propionate and ethyl isobutyrate hydrolyses were also performed. The results obtained, which displayed little temperature dependence, did

not agree with those of Halevi. The observed $k_{unlabeled}/k_{heavy}$ ratios are:

Temp	5.00°	15.00°	20.05°
$k/k_{\text{acetate-}\underline{d}_3}$	0.959±0.010	0.968±0.012	0.958±0.005

Temp	25.00°	29.80°	35.00°
$k/k_{\text{acetate-}\underline{d}_3}$	0.9623±0.006	0.974±0.005	0.970±0.004

Temp	45.01°	50.09°	60.00°
$k/k_{\text{acetate-}\underline{d}_3}$	0.967±0.008	0.970±0.013	0.988±0.017

Temp	20.02°	30.00°	40.02°	50.02°
$k/k_{\text{propionate-}\underline{d}_2}$	0.936±0.024	0.946±0.011	0.949±0.006	0.982±0.016
$k/k_{\text{propionate-}\underline{d}_3}$	1.016±0.018	1.015±0.014	1.034±0.005	1.021±0.015

Temp	30.02°	40.03°	50.02°	60.01°
$k/k_{\text{isobutyrate-}\underline{d}_1}$	1.018±0.022	1.014±0.022	1.020±0.010	1.006±0.014
$k/k_{\text{isobutyrate-}\underline{d}_6}$	0.941±0.018	0.907±0.020	0.928±0.008	0.923±0.012

Activation parameters for each ester were calculated. The decrease in rate with substitution resulted from ΔS^*, not ΔH^*.

Explanations for the observed rate ratios based on a threefold barrier to rotation have been offered. The normal isotope effect observed for ethyl isobutyrate-d_1 hydrolysis is taken as evidence for a twofold barrier. Torsional effects have also been considered.

---

(1) M. L. Bender and M. S. Feng, *J. Am. Chem. Soc.*, **82**, 6318 (1960).

(2) E. A. Halevi and (Mrs.) Z. Margolin, *Proc. Chem. Soc.*, 174 (1964).

AN AUTOMATED ANALYSIS
OF SECONDARY ISOTOPE EFFECTS
IN
AQUEOUS ALKALINE ESTER HYDROLYSIS

By

William Charles Sass

A THESIS

Submitted to
Michigan State University
in partial fulfillment of the requirements
for the degree of

DOCTOR OF PHILOSOPHY

Department of Chemistry

1970

To my old and new families

ACKNOWLEDGMENTS

The author wishes to express his appreciation to Professor Gerasimos J. Karabatsos for his guidance and for his assistance in interpreting these data.

The financial support provided by the National Science Foundation and the Department of Chemistry, Michigan State University, is gratefully acknowledged.

Appreciation is also expressed to the author's wife, Evelyn, for her help in the preparation of this manuscript.

TABLE OF CONTENTS

Page

LIST OF TABLES

LIST OF FIGURES

HISTORICAL AND INTRODUCTION

It is generally accepted that kinetic secondary isotope effects are the result of force constant changes occurring between the ground state and transition state (1).

Figure 1 demonstrates the effect of force constant changes on the activation energy of unlabeled and deuterated compounds. A decrease in the transition state force constant, which corresponds to a widening of the potential well, is accompanied by a decrease in vibrational differences between the two compounds. Although by virtue of its higher vibrational frequency, the energy of the lighter compound still exceeds that of the heavier, the diminished difference will lead to a smaller activation energy and higher reaction rate for the unlabeled compound. This is the "normal kinetic isotope effect."

When initial or zero point energy (ZPE) differences are exaggerated in the transition state by an increased force constant, the heavier compound reacts faster. This is referred to as an "inverse kinetic isotope effect."

Since Lewis and Boozer (2) reported the first observed secondary isotope effect in 1952, an intensive search for the origin of the force constant changes has been conducted. In order to make quantative predictions it is necessary to have an accurate representation of both the ground state and transition state structures. While the former is generally obtainable by conventional spectroscopic measurements, the latter is not.

Figure 1 (a). Decreased Force Constants Resulting in Decreased Vibrational Differences.

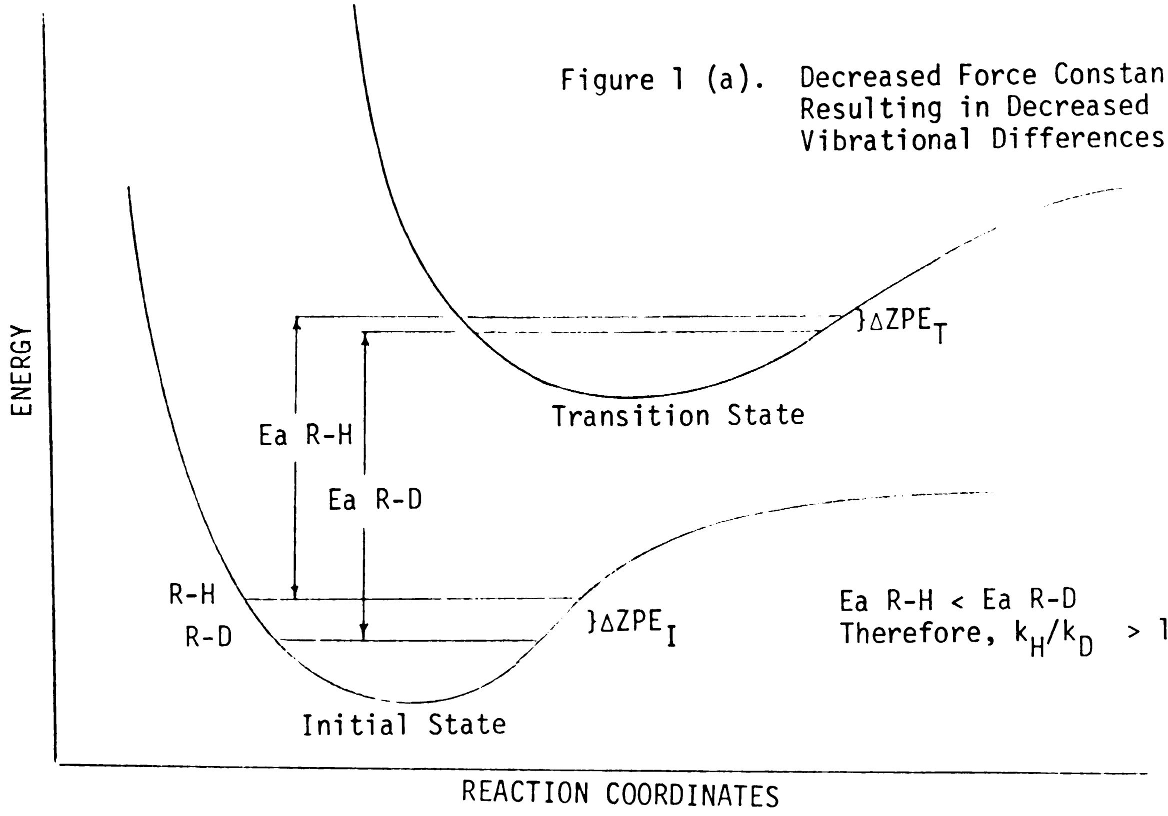

Figure 1 (b). Increased Force Constants Resulting in Increased Vibrational Differences.

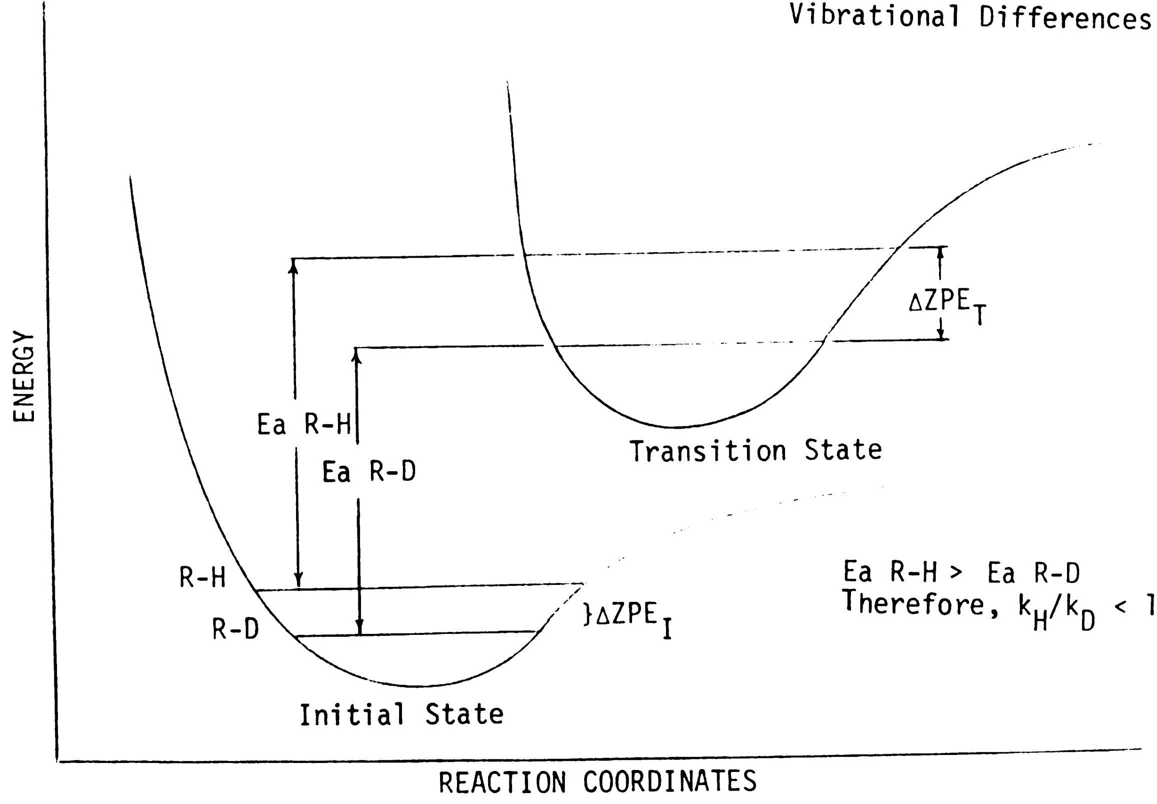

An empirical solution was presented by Streitwieser and coworkers (3). Force constants of a "carbonium ion like" transition state were assumed to resemble those of aldehydes. The trigonal sp^2 geometry of the aldehyde, along with its partial positive charge resulting from inductive effects of the oxygen, support the model.

The principal frequency change in going to the assumed transition state was a 550 cm^{-1} decrease in the out-of-plane carbon-hydrogen bending vibration. Since this corresponds to a k_H/k_D of 1.38, as compared to a typical observed value of 1.15 for an S_N1 α-effect, an explanation for the discrepancy must be sought. This explanation is as follows: The transition state is reached with the departing group still in the vicinity of the developing carbonium ion (Figure 2). If its presence were assumed to decrease the frequency difference $\nu_H - \nu_H^*$ to about 300 cm^{-1}, the discrepancy between the experimental and the calculated k_H/k_D value disapears.

It should be noted that this explanation is consistent with the absence of α-isotope effects in S_N2 solvolyses. Interference with the C-H bending by both incoming and leaving groups may lead to no frequency change and thus to no isotope effect.

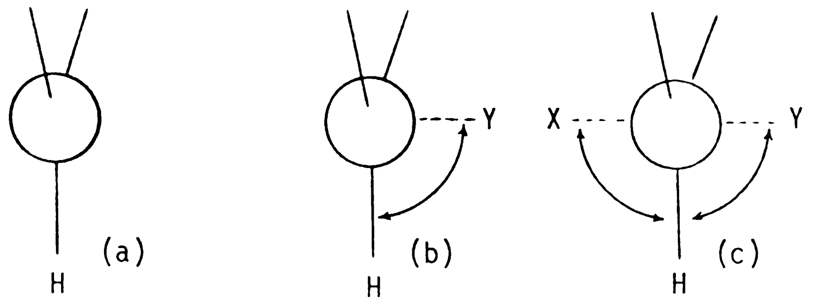

Figure 2. Interference to out-of-plane C-H bending motions: (a) in aldehydes, (b) in S_N1, and (c) in S_N2 transition states.

Various theoretical approaches to the transition state structure have been reviewed and compared by Weston (4).

Wolfsberg and Stern (1,5) have developed a computerized analysis of kinetic isotope effects based on the assignment of atomic weights, molecular dimensions, and arbitrary force constants to the initial and transition states. Their results confirm the assumption that both α and β isotope effects must be accompanied by force constant changes at the site of isotopic substitution. The authors (6) later reported that acceptable solutions may be approximated by "cutting off" (and replacing with a rigid comparable mass) portions of the molecule more than two bonds removed from the reaction site.

Despite general agreement that secondary isotope effects are caused by force constant changes, the origin of the change remains unclear. Extensive research has led to three interacting effects (7a). They are: hyperconjugation, an inductive effect, and a steric effect.

The principal parameters affecting hyperconjugation are the relative electronegativities of hydrogen and carbon, reflected in the Coulomb integral, and the tightness of binding of the electrons in the methyl group, reflected in the overlap integral. Although LCAO-MO calculations on systems containing fully formed carbonium ions are dominated by the Coulombic term (7b), it is not unreasonable to assume, in view of the shorter range of exchange forces than Coulomb forces, that in a reaction in which the carbonium ion is being formed by rupture of a CX bond, the effect manifests itself earlier on the overlap integral than on the Coulombic integral (7b).

As Streitwieser and coworkers (3) have indicated, the result of increased hyperconjugation in the transition state is reduced carbon-hydrogen (deuterium) force constants. This reduction (Figure 1) leads to normal isotope effects without recourse to preferential hyperconjugation by hydrogen.

Since the potential well, as illustrated in Figure 1, is unsymmetrical, the hydrogen, with its greater amplitude of vibration, will be characterized by a larger average bond length. The shorter mean CD bond length will result in a larger D...D repulsion. This increased repulsion enlarges the DCD bond angle. Intuitively, this leads to less p character in the C-D bond, thus making methyl-d_3 a better electron donor than methyl (7c).

It appears safe to generalize: (a) Increased transition state hyperconjugation stabilizes methyl more than methyl-d_3. (b) Methyl-d_3 donates electrons through the bonds better than methyl. (c) Methyl represents a larger steric bulk than methyl-d_3. Interpretation difficulties arise in part from the contrary nature of (a) and (b).

A fundamental paper by Shiner (8) firmly established the importance of hyperconjugation in kinetic isotope effects. The bicyclo compounds 1 and 2 and their unlabeled counterpart contain C-D(H) bonds which are respectively parallel to and orthogonal to the developing vacant orbital in the limiting solvolysis.

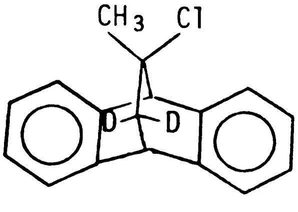

1

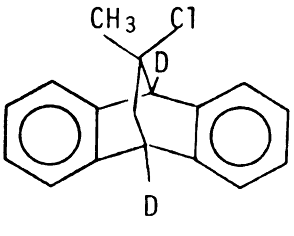

2

The predicted increased stabilization of the transition state of 1 by hydrogen hyperconjugation is supported by the observed rate ratio for 1 of k_H/k_D = 1.14.

The geometry of 2 prevents overlap by the labeled C-H bond. Absence of hyperconjugation results in an observed ratio of k_H/k_D = 0.986, presumably resulting from better inductive stabilization of transition state by deuterium.

A more recent paper by the same author (9) reports isotope effects in the acetylenic systems 3 and 4.

3 $(CD_3)_2\ CClC{\equiv}CCH_3$ 4 $(CH_3)_2\ CClC{\equiv}CCD_3$

k_H/k_D=1.655 k_H/k_D=1.092

Since inductive and steric forces cannot operate through such great distances, the effect must result from hyperconjugation acting through the π system of the acetylene.

The general concept of hyperconjugation is based on the Baker-Nathan order. It has been observed in many systems (10) that carbonium ion stabilization occurs in the following order: Me > Et > i-Pr > t-Bu > H. This series parallels the number of hydrogens available for hyperconjugation.

An opposite rationalization for this violation of the accepted inductive trend claims that the larger groups inhibit solvent stabilization (11). Serious doubts over this explanation have been raised by Berliner (12). In a review of the literature he showed that in at least 40 systems, para substituents followed the Baker- Nathan order in electrophilic reactions while substituents in the meta positions, from which conjugation is not possible, followed the normal inductive order, t-Bu > i-Pr > Et > Me, despite their closer proximity to the reaction site.

Based on the small rate differences observed in the Baker-Nathan series, Taft and Lewis (13) and Brown and coworkers (14,15) have suggested that some stabilization by carbon-carbon hyperconjugation is occurring. The importance relative to carbon-hydrogen hyperconjugation was calculated to be H/C = 1.3±0.1 and H/C = 1.25, respectively.

Perhaps the best view of the controversial question (16) of carbon-carbon hyperconjugation was recently expressed by Jensen and Smart (17). The authors indicate that the only unequivocable evidence for carbon-carbon hyperconjugation occurs in systems containing excessive p character in the carbon-carbon bonds. Para substitution by cyclopropane increases the rate of t-cumyl chloride (5) solvolysis by a factor of 157, while isopropyl substitution increases the rate by only 17.8.

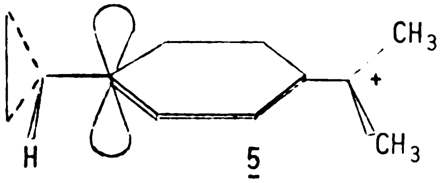

5

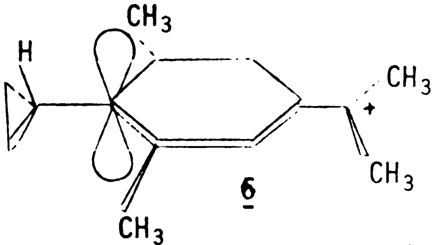

6

The rate enhancement, presumed to come from preferred C-C overlap in this strained system, can be substantially diminished by the effects to two added methyl groups (6) which sterically prevent the carbon orbital from becoming parallel to the π system. This results in a rate enhancement over the corresponding isopropyl substituted t-cumyl chloride by only a factor of nine. The importance of geometry for strained ring assistance in solvolysis has also been reported by Schleyer (17) in the cyclopropyl adamantyl system.

Halevi and coworkers (18), in a careful study of pKa values, have found a decrease in the acidity of deuterated aliphatic acids and benzylammonium ion, as shown below. They attributed this decrease to differences in the electronegativity of hydrogen and deuterium.

Table I. Acidity Reductions in Deuterated Acids.

Acid	ΔpKa
CD_3COOH	0.026
CH_3CD_2COOH	0.034
CD_3CH_2COOH	0.007
$PhCD_2COOH$	0.048
$PhCD_2NH_3^+$	0.054

Increased electron donation by deuterium over hydrogen was believed to destabilize the anion and cause the resulting decrease. Variation in dipole moment and polarizability of NH_3 (19), increased shielding of hydrogen (20) and fluorine (21) in nmr spectra by deuterium substitution, and chemical evidence such as the inverse isotope effect cited above by Shiner (8), are among the more compelling evidences supporting deuterium being more electropositive than hydrogen.

Brown and coworkers (22) have shown that in the Lewis acid-base neutralization reaction between boron trifluoride and 2,6-lutidine-d_6 (7), a stronger bond is formed than between the unlabeled species.

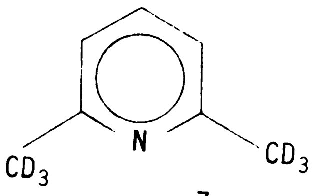

7

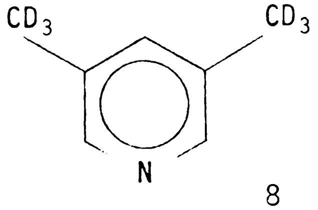

8

Absence of isotopic effects when 3,5-lutidiene (8) was used, based upon the difference in heat of reaction, tend to discredit inductive and hyperconjugative effects in this system. The authors attributed this isotope effect to non-bonded interactions. Further support for the presumed steric effect was also obtained when it was determined that trimethyl-d_9-boron formed a 25% stronger bond with ammonia than did the unlabeled compound in violation of the predicted inductive effect.

Mislow and coworkers (23) reported the observation of a purely conformational normal isotope effect of six per cent in the twisted D_2 ring system (9). Known not to proceed via enolization, the racemization of (9) became the first reported isotope effect not involving bond making or breaking.

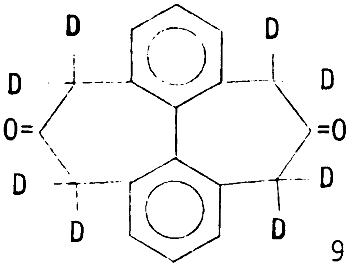

9

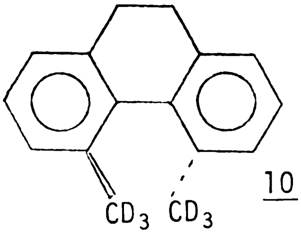

10

Mislow and coworkers (24) also reported another conformational kinetic isotope effect in the racemization of the sterically non-planar C_2 ring system (10). The larger steric requirements of hydrogen over deuterium are presumed to be responsible for the higher energy required to racemize the hydrogen compound.

Another example of nonbonded effects upon racemization kinetics was reported by Melander (25) in the C_2 system of 2,2′-dibromo-4,4′-dicarboxy-6,6′-biphenyl-d_2 (11). Part of the 18% inverse isotope effect observed for this system might have arisen from inductive differences between hydrogen and deuterium upon π orbital overlap. In consideration of this, the

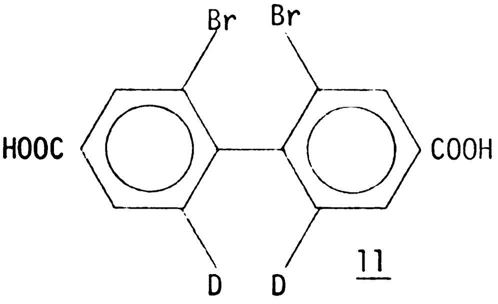

11

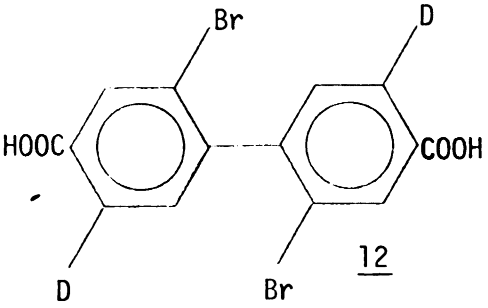

12

corresponding biphenyl with deuterium in the $5,5'$ position (12) was synthesized (26). Racemization yielded no isotope effect outside experimental error (1.02 ± 0.02).

H. C. Brown (22) has stated that virtually all deuterium isotope effects may be best described in terms of steric differences. L. S. Bartell (27) has gone beyond this and claimed that even such physical phenomena as the shorter bond lengths and the smaller than predicted bond angles in alkenes obtained by electron defraction studies (28) may be explained by nonbonded interactions without recourse to hybridization or hyperconjugation effects.

Work in this laboratory by Dr. Sonnichsen (29) compared experimental values with those predicted by Bartell's model (30). The system studied was the family of 1-naphthoyl chlorides and methyl esters with H, D, CH_3, and CD_3 substituents in the eight position. In this system, which precludes hyperconjugation, satisfactory results between experimental and calculated isotope effects were obtained. Predictions were not as satisfactory, however, in *t*-butyl-*d*$_9$ chloride, ethyl acetate-*d*$_3$, and acetyl-*d*$_3$ chloride, where hyperconjugation can occur.

Excluding special conformational factors (8), the reduction in the β-CH force constant in the activation process of limiting solvolysis appears to be related to hyperconjugative interaction with the developing vacant orbital. Despite the arguments already presented supporting a steric interpretation of isotope effects, it should be noted that they generally appear only when hyperconjugation is precluded or highly hindered species (23,24,25) are involved.

The solvolyses of 3-pentyl brosylate, 2,4-dimethyl-3-pentyl brosylate, and their β deuterated analogs were examined by Shiner and Stoffer (31).

The observation of cumulative effects in the former as one proceeds from the unsymmetrical doubly deuterated to the tetra-deuterated species ($1.3171 \approx \sqrt{1.7365}$) was interpreted as indicating a hyperconjugative effect. The difference in isotope effect resulting from mono and dideuteration of the latter compound ($1.3671 > \sqrt{2.1179}$), however, indicates that irregularities are occurring, probably resulting from participation.

The importance of the leaving group on the magnitude of secondary isotope effects has recently been emphasized by Shiner and coworkers (32) in the solvolyses of meta and para substituted 1-phenylethyl chlorides and bromides and their α-$\underline{d}$ and β-$\underline{d}_3$ analogs. The 15% α isotope effect observed upon chloride solvolysis was unaffected by H, meta-methyl, para-fluoro, para-phenoxy, and para-methoxy substituents. It was concluded therefore that all solvolyzed by a limiting mechanism. Progressively smaller β effects observed in the same series for compounds more reactive than 1-phenylethyl chloride were attributed to a reduction in the demand for hyperconjugation. Despite the similarity of the mechanism for the chlorides and bromides solvolyses, as evidenced by their similar β isotope effects, the bromide α effect was three per cent lower than the corresponding chloride. The difference is a reflection of weaker ground state bending force constants in the bromide.

Trifluoroethanol, with its high ionizing power and low nucleophilicity, has found acceptance (33) as a solvent favoring a limiting mechanism without posing the difficulties to precision conductance measurements that acetic and formic acid do. In the above paper, Shiner and coworkers also reported the same rate ratios for p-methylbenzyl-α-$\underline{d}_2$ chloride in 94% trifluoroethanol-water (1.146 per D) and 70% trifluoroethanol-water (1.140) as had been reported for α-phenylethyl-α-$\underline{d}$ chloride in various ethanol water mixtures (1.146-1.153).

The contrast between the similarity of rate ratios observed in structurally different chlorides and the lower isotopic rate ratios (by three per cent) of each of the corresponding bromides led the team composed of Shiner, Rapp, Halevi, and Wolfsberg (34) to postulate that the leaving group, and not the alkyl group, dominates the α-isotope effect in limiting reactions. Their calculations, which were based on transition state theory, assumed comparable bond strengths in the transition state for various halides. The correspondence between experimental and calculated results supports their hypothesis (35) that ground state differences are the source of variation in α k_H/k_D effects in limiting solvolytic reactions.

In a study of incoming and leaving groups, Jackson and Leffek (36) evaluated the rate ratios obtained in thiosulfate displacement reactions on methyl bromide, iodide, methanesulfonate, and p-toluene sulfonate. The rate ratio for methyl p-toluenesulfonate (1.12) is of special significance since it is the largest reported isotope effect observed to date in nucleophilic displacement reactions. They added their results to the correlation proposed by Seltzer and Zavitsas (37). This is an observed linear relationship between the k_H/k_D values and the difference in nucleophilicity of the incoming and leaving groups. The explanation given for the relationship, based on Hammond's postulate (38), is that a good incoming nucleophile will make little bond at the transition state. Thus, the decreased steric requirements (or decreased force constants) result in a normal isotope effect. Conversely, a weak incoming nucleophile will be extensively bonded at the transition state and thus lead to an inverse isotope effect. Between these two extremes, incoming and leaving groups of comparable nucleophilicity are predicted by Seltzer to lead to no isotope effect.

In an attempt to verify this latter prediction, Seltzer and Zavitsas (37) measured the α isotope effect in the displacement of methyl iodide with isotopic sodium iodide. Their results in methanol (1.05) and in water (1.10) were far from the predicted value of 1.00. In order to rationalize these numbers, they postulated a symmetrical energy profile containing two peaks. The first transition state was reached with little bond making or breaking. As the incoming group moved in closer, stability increased leading to a symmetrical intermediate. Stretching of the second bond raised the energy to the second transition state and finally to products.

In the preceding discussions, extensive reference has been made to the importance of substrate structure and conformation of the alkyl group on secondary kinetic isotope effects. The significance of entering and leaving groups has also been mentioned. So far, few references have been made to solvation effects, even though all the preceding reactions were performed in solvent. The neglect of solvation effects is due not to their unimportance, but to the unfortunate lack of quantitative information regarding these effects.

Hakka and coworkers (39) have reported that a 25° temperature increase decreases the isotope effect in the solvolysis of t-butyl-d_9 chloride by ten per cent. This decrease was shown to be the result of the activation energy being dominated by enthalpy: $\ln(k_H/k_D) = -\Delta\Delta H^*/RT + \Delta\Delta S^*/R$. The small observed values of ΔS^* (in 50% ethanol-water = -2.8 eu; in water = +14.5 eu) indicates only slight changes in solvent order between the ground state and transition state. Since extensive solvation of the cation would lead to a highly ordered transition state, the authors concluded that the transition state was reached when solvation was just beginning.

Previously, the opposite effect (temperature independence of k_H/k_D) (40) was observed for the solvolyses of isopropyl methanesulfonate, tosylate, and bromide and their $\underline{d}_6$ analogs. From the difference in the activation parameters in Table II, it can be seen that at normal temperatures, entropy differences dominate $\Delta\Delta G^*$. The activation values were obtained by plotting log k_H/k_D versus 1/T.

Table II. Activation Differences Between Labeled and Unlabeled Isopropyl Derivatives.

$$\log_{10} k_H/k_D = \frac{(\Delta H^*_D - \Delta H^*_H)}{2.303RT} - \frac{(\Delta S^*_D - \Delta S^*_H)}{2.303R}$$

	$\Delta\Delta H^*$(cal/mole)	$\Delta\Delta S^*$ (eu)
i-Pr SO_3Me	7±28	-0.84±0.1
i-Pr OTs	-21±14	-0.93±0.05
i-Pr Br	-35±15	-0.65±0.05

Although it has been suggested that isotopic substitution may affect solvation (41,7), it is generally accepted that the isotope effects reflect differences in enthalpy. Leffek (40) has suggested that the entropy difference results from changes in internal rotation barriers. Microwave studies (42) have indicated that ground state barriers are six per cent lower in acetone-$\underline{d}_6$ than acetone and ten per cent lower in nitromethane-$\underline{d}_3$ than in unlabeled nitromethane. Taking into account these differences in ground state barriers for the labeled isopropyl compounds, and arbitrarily choosing small barriers in the transition state for both compounds, Leffek and coworkers (40) calculated the following:

Table III. Calculated Activation Differences Between Labeled and Unlabeled Isopropyl Derivatives.

Assumed Barriers (cal/mole)			Calculated Activation Values	
H Ground State	D Ground State	Transition State (both)	$\Delta\Delta H^{*}_{D-H}$ (cal/mole	$\Delta\Delta S^{*}_{D-H}$ (eu)
3000	2400	0	-93	-0.26
3000	2400	600	-31	-0.26
3000	2400	1200	-44	-0.26

The direction of these effects would tend to cancel the normal enthalpy difference while creating an entropy difference.

As an alternate explanation, Robertson (39) has pointed out that the lack of temperature dependence in isotope effects may result from interference by the incoming nucleophile which raises the torsional and bending frequency of the methyl bond. Charge may still develop in the transition state and be reflected in a decrease of high frequency stretching vibration when charge dense oxygen or chloride are the leaving groups. Opposing changes in bending and stretching vibrations may thus make $\Delta\Delta H^{*}$ very small.

Explanations have thus been offered to explain entropy differences with or without recourse to solvation.

Robertson (43) has emphasized the importance of ground state solvation. It has already been pointed out (39) that <u>t</u>-butyl chloride solvolysis results in a transition state in which solvation is only beginning to become important. This conclusion is based largely on the negative heat capacity changes which often accompany ionogenic reactions. From the definition of enthalpy, $H = \int C_p dT$, it can be seen that the heat capacity is the coefficient of the temperature dependence of enthalpy.

Heat capacity differences are the best available probe with which to investigate solvation effects. In a study of the effects of varying solute concentrations in water, Robertson and Sugamori (44) studied the effects of solute addition on ΔC_p^*, the difference between ground state and transition state heat capacities, in the aqueous solvolysis of t-butyl chloride. Solute addition initially resulted in increasingly more negative values for ΔC_p^*. A minimum was reached, however, beyond which the values increased.

The observed decrease in ΔC_p^* implies that solute improves the solvation of the ground state relative to that of the transition state up to a point. Excess solute finally begins to hinder the improved solvation. The solutes studied were ethanol, isopropyl alcohol and t-butyl alcohol. A plot on ΔC_p^* versus the mole fraction of solute revealed that the maximum appeared in the opposite order. Further, it was shown that the maximum corresponded to the same "volume of alkyl group" in the three cases. It was thus concluded that the solute improves the ground state solvation until all the "holes" in the "frozen" water solvent cage were filled. Beyond this point, the solute inhibits aqueous solvation.

Heat capacities of activation have been utilized by Blandamer and coworkers (45) as a mechanistic probe. Limiting reactions frequently have ΔC_p^* values which are 20 cal/mole more negative than nucleophilic reactions. The authors studied the effects of solvent reorganization and anchimeric assistance on ΔC_p^* values. They were able to show that several of the reactions were limiting even though their products suggested a bimolecular reaction.

Results in this (46) and other laboratories (36,47) have indicated that some secondary isotope effects may be highly temperature dependent. A temperature study by Karabatsos and coworkers (56) of isotope effects in the limiting solvolysis of 8-methyl-$\underline{d}_3$ naphthoyl chloride and its unlabeled analog displayed a substantial difference in the 13 and 17% isotope effects observed at -26.6° and -34.0°, respectively, and the 2.9% isotope effect observed at 25°.

Bender and Feng (48) found ethyl acetate-$\underline{d}_3$ to hydrolyze 10% faster at 25° in aqueous base than its unlabeled analog. This isotope effect, which may be explained by greater hyperconjugation in the ground state than in the transition state, was incorporated in the temperature study on the same compounds by Halevi and Margolin (47). Their results, along with that of Bender and Feng, are given below:

Temperature	0°	25°	35°	65°
k_H/k_D	1.00±0.01	0.90±0.01	0.93±0.01	1.15±0.09

This temperature dependence, Figure 3, is unprecedented for secondary isotope effects. The occurrence of a minimum at the temperature "...where the disassociation of weak alphatic acids, such as propionic and butyric, take on maximum values [is interpreted as] evidence that small differences in energy and entropy of solvation, resulting from isotope differences in average charge distribution, largely determine the secondary isotope effects in this and other highly aqueous systems" (47).

Clearly, if correct, the temperature dependence of this reaction has important consequences for the interpretation of isotope effects determined at a single temperature. The reported results are sufficiently significant that they warrant additional confirmation.

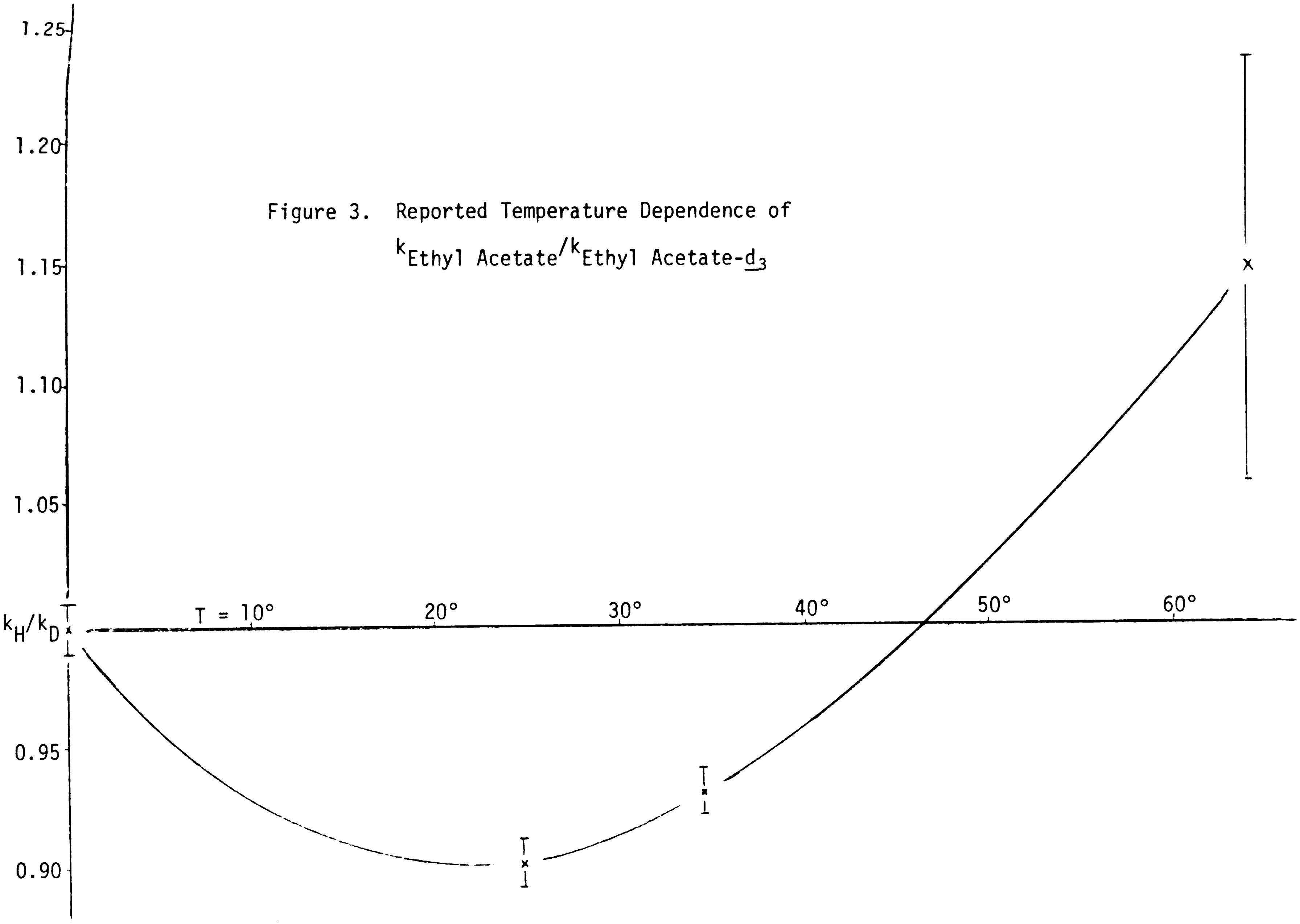

Figure 3. Reported Temperature Dependence of $k_{\text{Ethyl Acetate}}/k_{\text{Ethyl Acetate-}\underline{d}_3}$

To this point, no mention has been made of the analytical techniques employed in gathering the preceding data. The number of techniques employed is sufficiently limited to allow them to be summarized:

(A) Changes in conformation (23-26) were followed by loss of optical activity.

(B) Differences in pKa of acids (18) were determined by differential pH measurements. That is, the effect of aliquots of base on pH near the one half nutralization point were compared, thus eliminating activity errors. Benzylammonium ion (17) was analyzed by ultraviolet spectroscopy.

(C) The solvolysis of various <u>meta</u> and <u>para</u> substituted <u>t</u>-cumyl chlorides (12,13), the acetolysis of ethyl trifluoromethane (49) sulfonate, as well as ethyl acetate hydrolyses (47,48), were followed by quench and titrate studies. The faster formolysis of ethyl trifluoromethane sulfonate (49) was followed by nmr.

(D) Iodide exchange (37) was followed by the increase in radioactivity in extracted aliquots of methyl iodide.

(E) In all other cases, the kinetics were followed by conductance, or no reference to technique was made.

Two of the conductometric techniques warrant special attention. Hyne and Robertson (50) compensated for the small nonlinearity observed in conductance measurements by utilizing the conductance bridge as a null detector between two cells. As substrate reacted in one cell, the system was balanced by adding to the other standardized electrolyte similar to that which was being generated. Time versus buret readings was recorded.

A fully automated bridge and data recording system has been employed by Robertson and Sugamori (44). At pre-selected intervals, the bridge balances itself, notes the time of balance on its internal digital clock, prints the conductance and time on a digital readout, and punches the same information on paper tape for later processing. The system can simultaneously monitor several cells. This latter technique offers a welcome relief from the drudgery of conventional kinetics.

The work presented in this thesis is a study of the effects of temperature on the aqueous alkaline hydrolysis of ethyl acetate-$\underline{d}_3$, propionate-$\underline{d}_2$ and $\underline{d}_3$, and isobutyrate $\underline{d}_1$ and $\underline{d}_6$, and their unlabeled analogs; the techniques applicable to such studies; and an interpretation of these temperature effects. It represents the continuing effort in this laboratory to better understand the origins and implications of secondary isotope effects.

RESULTS AND DISCUSSION

I. Selection Of The System

A study of isotope effects in the alkaline aqueous hydrolysis of simple aliphatic esters would have been a potentially significant study even without the unusual temperature dependence reported by Halevi and Margolin (47).

Alkaline ester hydrolysis, the mechanism of which is discussed in more detail below, is known to proceed via a rate determining attack of base. The rate of the reaction is thus determined by the transformation of a neutral ground state possessing some carbonium ion characteristics 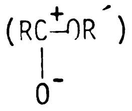 $(\mathrm{R}\underset{\mathrm{O}^-}{\underset{|}{\overset{+}{\mathrm{C}}}}\!-\!\mathrm{OR}')$ into a tetrahedral anion, the charge of which is localized on the carbonyl oxygen. In two respects this is the reverse of a limiting solvolysis. First, substituents on the carbonyl experience a decrease in their intially positive environment, and second, the transition state has become more crowded rather than less.

This general discription suggests two other potential interesting systems. The first is the series of base catalyzed condensation reactions in which the breaking of CD bonds is avoided. Here also, secondary effects will reflect a more crowded anionic transition state. To the author's knowledge, no such study has been performed. Experimental difficulties elaborated in Part II, Analytical Methods, may suggest the reason. The second system involves the effect of deuteration on the attack of Grignard upon carbonyl and related groups. Regrettably, the mechanistic state of the art involving Grignard reagents is such that this potentially interesting study is at present impossible. Yields are unreproducible and there even exists disagreement as to whether the kinetic order of the Grignard is two (51) or three (52). Ashby and coworkers (52) in a study of side reactions report:

> The increase in by-product formation with an increase in Grignard to ketone ratio leads us to believe that benzopinacol formation is caused by small amounts (PPM) of transition metal impurities known to exist in triply sublimed magnesium.

In contrast with the above difficulties, the ester hydrolysis mechanism has been well established.

The kinetic order of two for the alkaline hydrolysis of esters was established nearly a century ago (53). This order and results of oxygen labeling studies are consistent with the following mechanism:

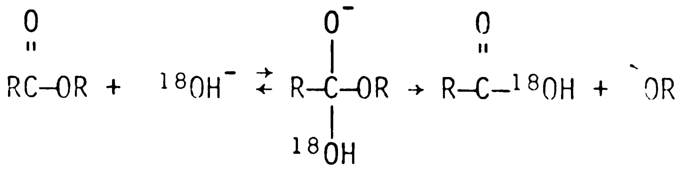

$$\overset{\overset{O}{\|}}{RC}\text{—}OR + {}^{18}OH^{-} \rightleftarrows R\text{—}\overset{O^{-}}{\underset{{}^{18}OH}{C}}\text{—}OR \rightarrow R\text{—}\overset{\overset{O}{\|}}{C}\text{—}{}^{18}OH + {}^{-}OR$$

13

The question arises as to whether 13 is an intermediate or a transition state. As a result of oxygen labeling experiments conducted by Bender (54), Moffat and Hunt (55) proposed the reaction scheme indicated in Figure 4.

Following the rate determining attack of hydroxide (k_1), the tetrahedral species may revert to starting material (k_2), or decompose to products (k_3). The decomposition may occur before or after proton exchange.

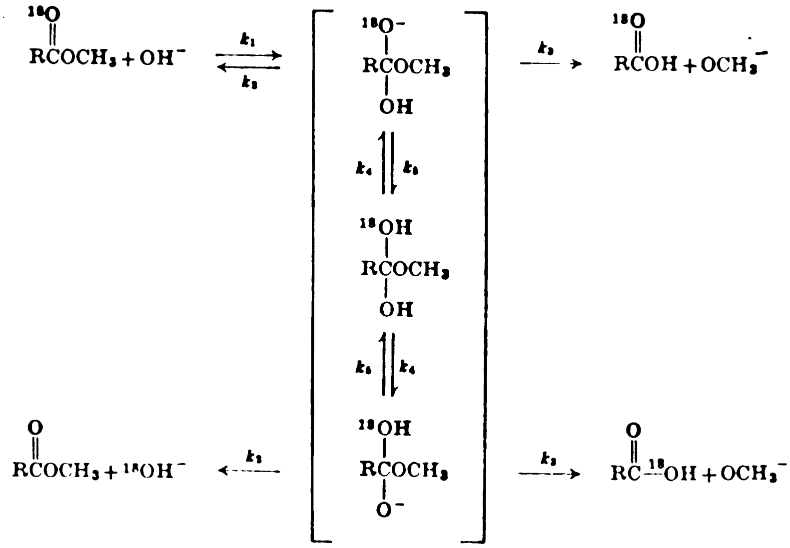

$$\frac{k_h}{k_e} = \frac{2k_3}{k_4}\left[1+\frac{k_3}{k_2}\right]+2\left[\frac{k_3}{k_2}\right]$$

Figure 4. The Significance of Protonation Kinetics on the Hydrolysis to Exchange Ratio.

If the protonation-deprotonation steps are fast, the hydrolysis to exchange ratio reduces to $k_h/k_e = 2k_3/k_2$. The effect of substituents on k_3/k_2 is expected to be small; the main effect occurs in k_3/k_4. Both rates should be increased by electron donating substituents, but k_3, which is one bond closer, should be more strongly affected. Table IV reflects the effects of varying substituents where R = p-XPh–.

Table IV. Substituent Effects on the Hydrolysis to Exchange Ratio.

X	σ	k_h/k_e
NH_2	-0.66	30±4
CH_3	-0.170	11±2
H	-0.00	5.7±0.8
C l	+0.226	6.3±1.10
NO_2	+0.778	2.8±0.3

Although the lifetime of the tetrahedral species must be extremely short to allow hydrolysis to compete with rapid proton exchange ($k_3 \approx k_4 \approx 10^9$ sec^{-1}), the occurrence of exchange indicates that the intermediate has a lifetime significantly greater than 10^{-13} second, the time required for a molecular vibration (56), and as such may be considered an intermediate.

It has been reported by Johnson (56) in his review of nucleophilic catalysis of ester hydrolysis and related reactions that k_1 is the slow step in acidic, neutral, and alkaline hydrolysis of oxygen esters, in the acidic hydrolysis of amides and anhydrides, and in the neutral hydrolysis of anhydrides, acid halides, and acetylimidazolium ion. Only in the alkaline hydrolysis of amides has k_3 become the slow step.

The effects of electronegativity and crowding on alkaline hydrolysis rates are indicated in Table V (57).

Table V. Substituent Effects on Alkaline Ester Hydrolysis Rates.

	CH_3COOMe	$CH_2ClCOOMe$	$CHCl_2COOMe$
$\frac{k}{k_{MeOAc}}$	1.0	761	16,000

	$(COOMe)_2$	CH_3COOEt	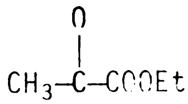 $CH_3-C(=O)-COOEt$
$\frac{k}{k_{MeOAc}}$	170,000	0.60	10,000

	CH_3COOEt	C_2H_5COOEt	$(CH_3)_2CHCOOEt$	$(CH_3)_3CCOOEt$
$\frac{k}{k_{EtOAc}}$	1.0	0.47	0.10	0.011

	CH_3CH_2OAc	$(CH_3)_2CHCH_2OAc$	$(CH_3)_3CCH_2OAc$	$(C_2H_5)_3CCH_2OAc$
$\frac{k}{kEtOAc}$	1.0	0.70	0.18	0.031

While it could be argued that some of the rate inhibition by alkyl substitutions on the acid could result from inductive effects of the substituents, the effect of substitution on the alcohol moiety must be steric in nature since the alteration is too far (four bonds removed) from the reaction site.

The deuterium isotope effect on alkaline ester hydrolysis is therefore an ideal system for study, because of the preliminary indications of an unprecedented temperature dependence, its "reverse nature" in comparison to limiting solvolysis, and its irreversible hydrolysis known to proceed <u>via</u> a single mechanism for which the rate determining step has been established.

II. Analytical Methods

Regrettably, many common techniques are inapplicable to this potentially valuable system. As noted earlier, most isotope effects have been determined by conductance measurements. Solvents are generally nonaqueous and initially contain no ionic species. Application of conductance measurements in such solvents as acetic acid are generally avoided because the self-ionization of the solvent introduces a significant initial conductance thereby reducing accuracy (33).

An examination of the stoichiometry of the ester hydrolysis reveals that it would require not the usual following of the sum of the conductances of the ions generated, but only the difference in conductance between hydroxide and acetate. While this difference is measurable, it represents a substantially smaller change superimposed on larger conductances than is generally measured and will result in a correspondingly lower resolution.

Ultraviolet Spectroscopy with the commercial availability of thermostated cells, has become a convenient technique for following kinetics. Although esters contain a chromophore, the carbonyl must be conjugated with an unsaturated system before the extinction coefficient becomes significant. The extinction coefficients of acetic acid and ethyl acetate are 32 and 57 at λ_{max} = 208 and 211 nm, respectively. This contrasts with an extinction coefficient of 13,500 at λ_{max} = 206 nm (53) for <u>cis</u>-crotonic acid 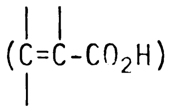 $(\overset{|}{\underset{|}{C}}=\overset{|}{C}-CO_2H)$ in the same solvent (ethanol). Clearly, ultraviolet spectroscopy is inapplicable to kinetic measurements in this unconjugated system.

Olah and Streitwieser (59, 49), among others, have applied nmr spectroscopy to kinetic measurements. Unfortunately, the tendency of the nmr to drift and the difficulty in measuring and maintaining accurate temperatures make this technique less than ideal.

Competition studies between labeled and unlabeled species have been widely applied (60,61). Application to this system would involve the hydrolysis of a known ratio of labeled and unlabeled ester. Aliquots are periodically withdrawn, quenched, and the ester extracted. Mass spectral or nmr analysis of unreacted ester will reveal the relative quantities of each remaining at various times from which the kinetic ratio k_H/k_D may be calculated. One advantage of this technique is that isotopically pure starting materials are unnecessary. One general disadvantage not applicable to this system is that isotope effects subsequent to the rate determining step may divert unequal portions of labeled and unlabeled material down alternate mechanistic paths leading to other products, thereby invalidating a study based on product ratio analysis. In addition to its tedious nature, competition was ruled out for this study, since only relative and not actual rates are revealed.

Having eliminated most of the common techniques by which substrate disappearance could be monitored, one seeks alternate techniques. As the ester hydrolyzes, one mole of base is consumed for each mole of ester that reacts. This formed the basis for the two preceding kinetic studies mentioned (47,48). Both consisted of quenching and titrating aliquots of reaction mixture.

In addition to the extremely tedious nature of titration studies involving the proposed analysis of the eight labeled and unlabeled esters at a total of 17 temperatures with three to six independent determinations each, it was desirable to know as many points as possible along the reaction path. Continuous methods of analysis were therefore considered.

Commercially available pH stats are capable of monitoring the kinetics of reactions in which acid (or base) is generated or consumed. Although pH stats may be used to follow kinetics of acid forming or consuming reactions, the technique involves experimental difficulties. The error signal resulting from deviation from the preset point drives a proportional rate pump to restore the balance. This implies that by virtue of the fact that titrant is being added, the solution is necessarily not at the preset pH; the instrument is not a "pH stat." It should be noted that errors as small as 0.05 and 0.01 pH units result in 13% and 2.6% errors, respectively. It was thus desirable to design a pH stat which would avoid the consistent deviation from the preset point. The author designed and built an analog integrating servo system which avoided this difficulty. The circuit is shown in Figure 5.

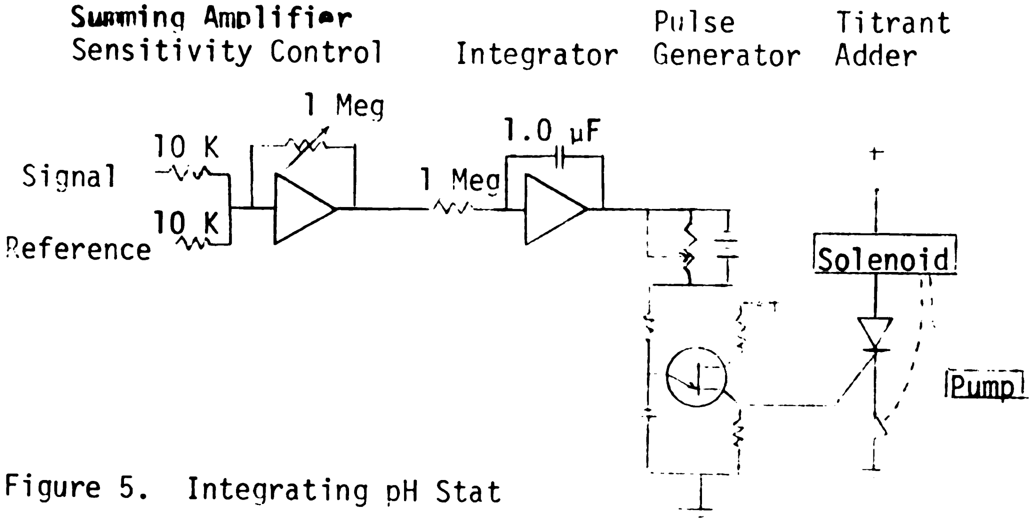

Figure 5. Integrating pH Stat

As the signal begins to deviate from the reference, this error signal begins to charge the integrating capacitor. Charge (and thus addition rate) increases with time, until addition is occurring at a rate which will curtail further drift. The error signal now existing, however, continues to charge the integrating capacitor, resulting in ever faster addition until the error signal has been forced back to zero. At this point the charge ceases to grow, but the existing charge overdrives the titration until the negative error signal subtracts enough charge to slow the addition rate to that of the reaction rate. A situation opposite that above now exists and the negative error signal continues to remove charge until the reaction rate exceeds the addition rate and the solution returns to the preset point from the negative. These oscillations are shown in Figure 6 for the case of 35 μl ethyl acetate in 15 ml 0.005 N KOH (K≈0.11 l/mole sec). The result is a 0.015 maximum pH deviation with 0.00 average deviation.

It is noteworthy that the amplitude of the maximum deviations (which correspond to the points at which addition rates just compensate for the effects of the reaction) decreases as the reaction slows. The result is a dampened sign wave with an average value coinciding with the preset value.

Although the analog system functioned well under test conditions, it contained two defects. First, any small offset voltage will continually be integrated, thus making the analog system prone to drift with time. Second, it is not adequate to have the pH value average the selected setting; it is the $[H^+]$ which must average a constant. Since the two are exponentially rather than linearly related, one does not imply the other. The latter deficiency may be corrected by inputting

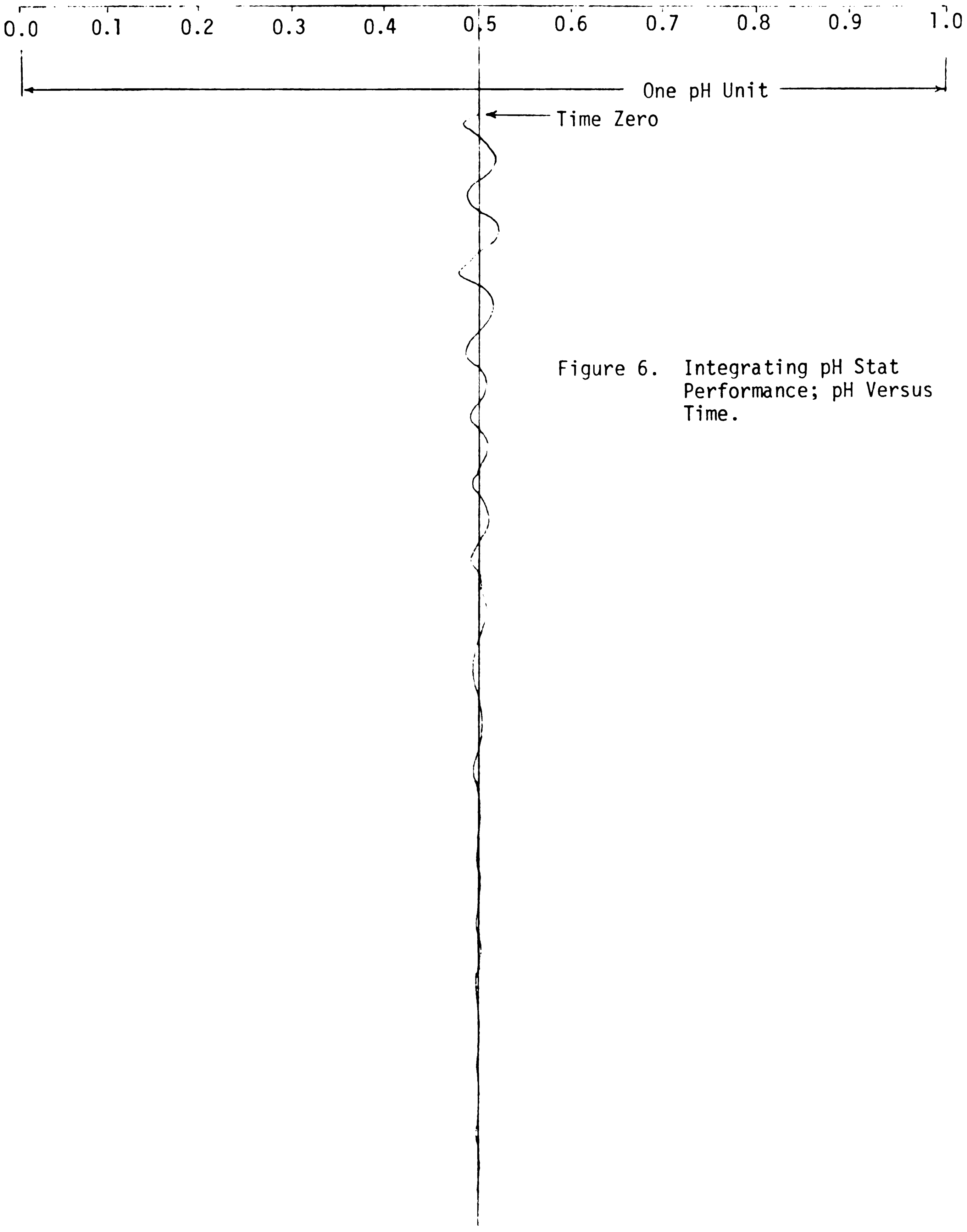

Figure 6. Integrating pH Stat Performance; pH Versus Time.

the pH through an exponential amplifier, but the former defect is inherent to the analog system.

Drift problems may be eliminated by replacing the entire analog system with the analogous digital system, since digital instruments are free from drift. It has been suggested by Professor Enke (62) that another way to eliminate the error signals characteristic of conventional pH stats might be to develop a digital system, interfaced to a titrant addition, which "remembered" its history. That is, to develop a system where the size of each aliquot of titrant is determined by the effect of the last three or so titrant additions. In this way, the device would quickly find the aliquot size required to just compensate pH changes caused by the reaction and no more. As the reactants vanish, the aliquot size would continually decrease, thereby avoiding both undershoot at the beginning overshoot at the end.

The "ultimate" pH stat may well be a combination of these two systems. Integration would offer a method of correcting for initially incorrectly chosen aliquot parameters, while the variable aliquot size would maintain the pH once the correct size was determined. An additional advantage of such a system would be the storing and analyzing of the data obtained by the same digital system thus allowing direct analysis of the kinetic parameters. Also, additional variables such as temperature fluctuations, slow equilibria, or incomplete solubility may be internally compensated for. The precision syringe drive required to implement the above systems was constructed by the author, but conditions did not allow the development of the rest of the digital interface.

A variation on the principle of the pH stat was developed many years ago by Peters and Walker (63). Kinetics of the alkaline hydrolysis of mustard gas was followed using methyl red as an indicator. Standardized 0.01 N base was added until the indicator's initially pink color had turned yellow. The time required to return to pink was noted, at which time a known volume of base (1 or 2 ml) was added and the process repeated. Since the time required to consume a known quantity of base is proportional to the rate constant, the kinetics could be determined.

More recent applications of this technique have been reported (64,65). An automated null point device operating on this principle was constructed by Hendy and coworkers (64). When the potential of a glass electrode exceeded a preset trigger level, a fixed volume of titrant was added. The time between pulses was recorded automatically. The appeal of this technique is lessened somewhat by the fact that kinetics of reactions which are not zero order in base are complicated by the constantly changing base concentration. The increased availability of computers has minimized this objection.

It was mentioned above that errors such as temperature drift may be minimized by simply monitoring the deviation and allowing the computer to compensate for its effects on the rate. This same principle may be applied to the measurement of kinetics. Instead of constructing a "perfect" pH stat, deviations may simply be monitored and compensated for by the computer. An application of this principle in the extreme case formed the basis of the system chosen for this kinetic study.

If a pH meter is linearly calibrated as described below, it is capable of monitoring pH changes accurately over moderately large intervals. Since one mole of base is consumed for each mole of ester reacting, simply following the drift of pH with time offers a convenient and precise technique for following such reactions. The kinetic rate may be determined by a computer solution of the special second order equation I. Since the reaction is known to be first order in both base and ester, a knowledge of the instantaneous concentrations of each is required. In the absence of an infinity point, which is precluded by the long term instability of glass electrodes in base, this information is supplied by the computer from a knowledge of initial conditions. Initial ester concentration is dependent only on the volume of neat ester injected with a micro liter syringe into the constant volume of the base utilized. Initial base concentration is determined by multiple titration of samples from the base reservoir.

Monitoring the extent of reaction requires careful linear calibration of the pH meter. Traditionally, a pH meter was calibrated by an adjustment of a balance control which varied the offset voltage of the meter until the reading agreed with a known buffer near the desired pH. This process corresponds to that shown in Figure 7a. If a measurement in another pH region was desired, the meter was recalibrated with a second buffer.

By the addition of a pH slope control, which simply modifies the mv/pH ratio, substantial portions of the pH range may be linearly calibrated. The process is as follows: The pH is set as before, but to that pH value corresponding to the isoelectric point of the electrode. This is the point (usually near a pH of seven) at which the potential of the glass-reference combination is zero. Variations in the pH/mv slope will not affect this pivot point, thus enabling the adjustment of slope with a second buffer as indicated in Figure 7b.

Once the calibration of slope is complete, the meter is capable of providing reliable pH values over a substantial range. It should be

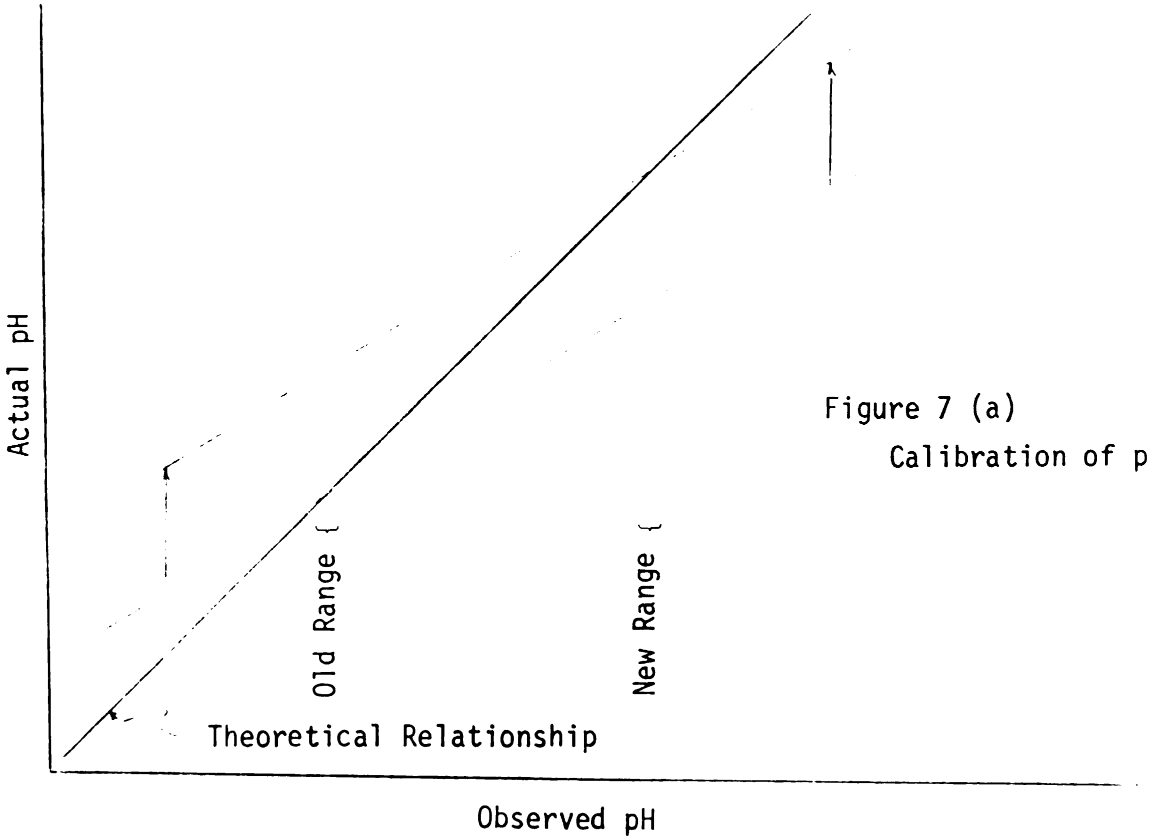

Figure 7 (a)
Calibration of pH

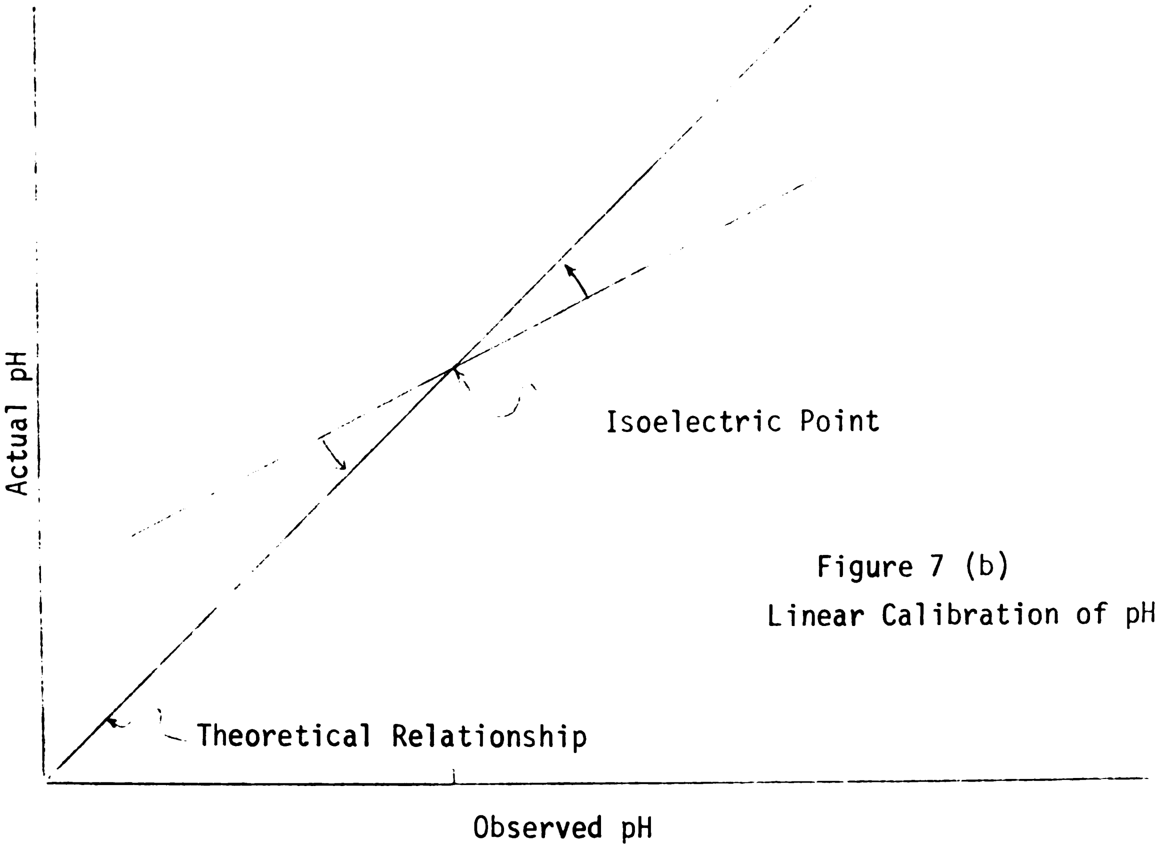

Figure 7 (b)
Linear Calibration of pH

further noted that a change in the balance setting will add a constant to the observed readings, but differences between successive readings remain accurate.

Setting the balance at the value of pH calculated from the relationship that $K_W = [H^+] [OH^-]$ and the assumption that pH = log $[H^+]$, the meter is now capable of following the change in base concentration from its initial value. The assumption that activities remain constant seem justifiable, since individual ion activities for all ions involved in this concentration range ($[OH^-]$ = 0.005 N) are 0.975 (66).

The output of the pH meter, adjusted as indicated, was recorded, digitized, and analyzed by a computer. The effectiveness of the technique is indicated by the consistent occurrence of correlation coefficients exceeding 0.999. A graph of typical data (kinetic run number 157, ethyl acetate-$\underline{d}_3$), is displayed in Figure 8. Also displayed is a typical computer print-out of the same data, Figure 9. In practice, ethyl propionate and ethyl isobutyrate kinetics were begun not at the pH value calculated, but at pH = 10.95. A constant correction factor was added. This modification removed the necessity of changing scale-expanded ranges in the middle of a kinetic determination.

Kinetic values, obtained for the eight esters, are tabulated in Tables VI through VIII. A summary of the rate ratios $k_{unlabeled}/k_{heavy}$ for the ethyl esters at 40°, calculated from a least squares analysis of the ratios versus temperature, is listed in Table IX. The choice of 40° was arbitrary. It represents the middle of the temperature range studied and as such reflects the least extrapolation error.

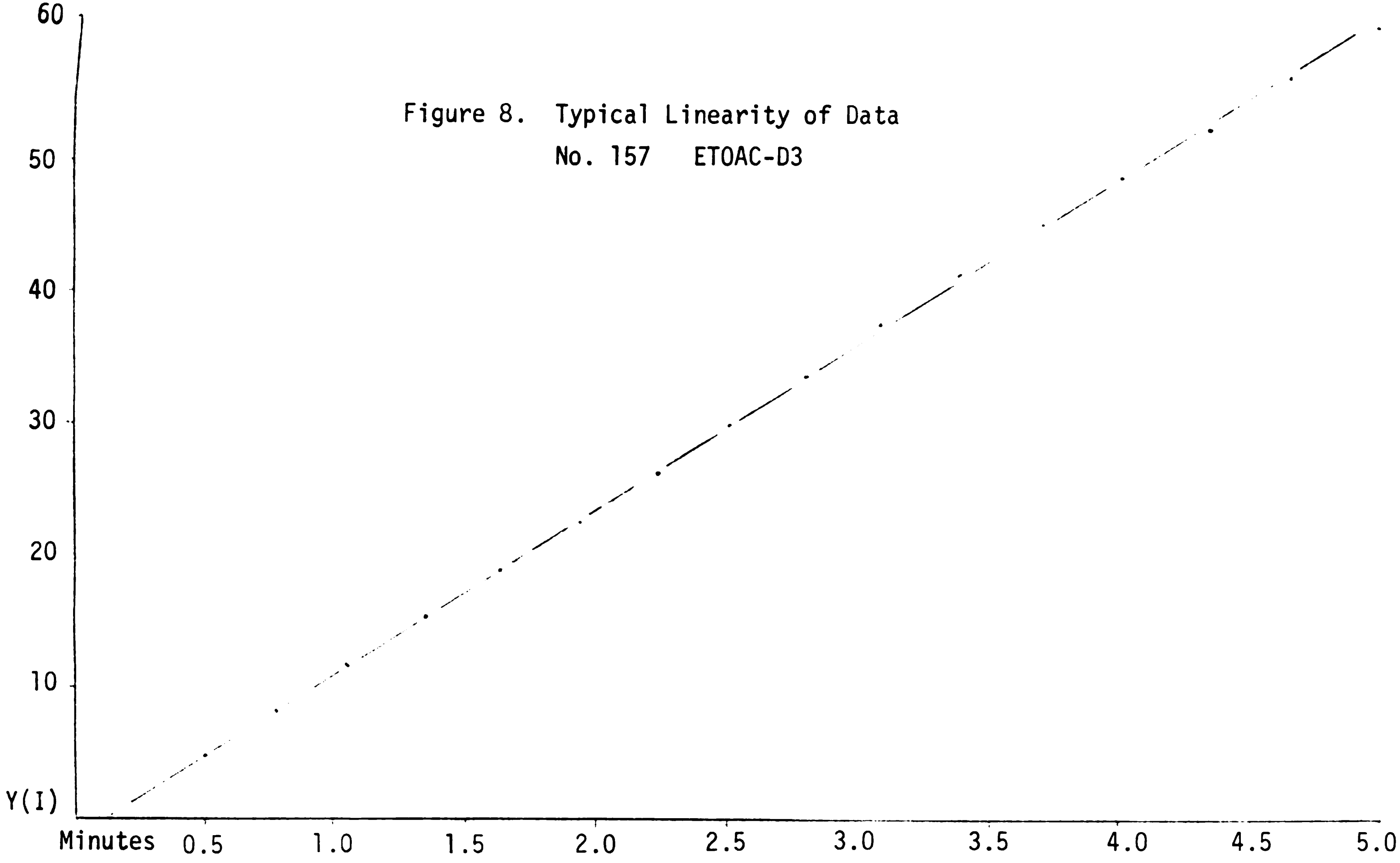

Figure 8. Typical Linearity of Data
No. 157 ETOAC-D3

Figure 9. Typical Computer Output

```
         NO. 157     E10AC-03    50 MICRO L  + 15 ML KOH    TEMP=35.000

    DEL I      T.MINUTES     PRESE    PH       H-ION CONCENTRATION         Y(I)          DELTA(I)

     .28          .50       11.25   11.2500       .56237E-11           .47559E+01      -.83168E-01
     .29          .78       11.20   11.2000       .63099E-11           .82455E+01      -.78299E-01
     .28         1.07       11.15   11.1500       .70795E-11           .11776E+02      -.15706E+00
     .28         1.35       11.10   11.1000       .79433E-11           .15344E+02      -.74153E-01
     .31         1.63       11.05   11.0500       .89130E-11           .18945E+02       .42574E-01
     .29         1.94       11.00   11.0000       .10001E-10           .22577E+02      -.18337E+00
     .28         2.23       10.95   10.9500       .11221E-10           .26237E+02      -.13261E+00
     .29         2.51       10.90   10.9000       .12590E-10           .29922E+02       .67750E-01
     .28         2.80       10.85   10.8500       .14126E-10           .33630E+02       .16635E+00
     .30         3.08       10.80   10.8000       .15850E-10           .37358E+02       .40987E+00
     .32         3.38       10.75   10.7500       .17784E-10           .41105E+02       .42291E+00
     .3[illegible]         3.70       10.70   10.7000       .19954E-10           .44868E+02       .20363E+00
     .31         4.0[illegible]       10.65   10.6500       .22388E-10           .48647E+02       .24815E+00
     .32         4.34       10.60   10.6000       .25120E-10           .52438E+02      -.67304E-01
     .34         [illegible]       10.55   10.5500       .28185E-10           .56242E+02      -.24630E+00
    1.00         [illegible]       10.50   10.5000       .31624E-10           .60056E+02      -.53898E+00
```

Figure 9. (Cont.)

```
SLOPE =    .207426E+00

STD. DEV. OF SLOPE =   .78[illegible]7E-03



INTERCEPT =  -.138371E+01

STD. DEV. OF INTERCEPT =     .142153E+00



STD. DEV. OF FIT =    .254303E+00



CORRELATION COEFFICIENT =    .9999



INITIAL ESTER CONCENTRATION =    .0338400000

INITIAL BASE CONCENTRATION =     .0043570000

KW =    .20893E-13
```

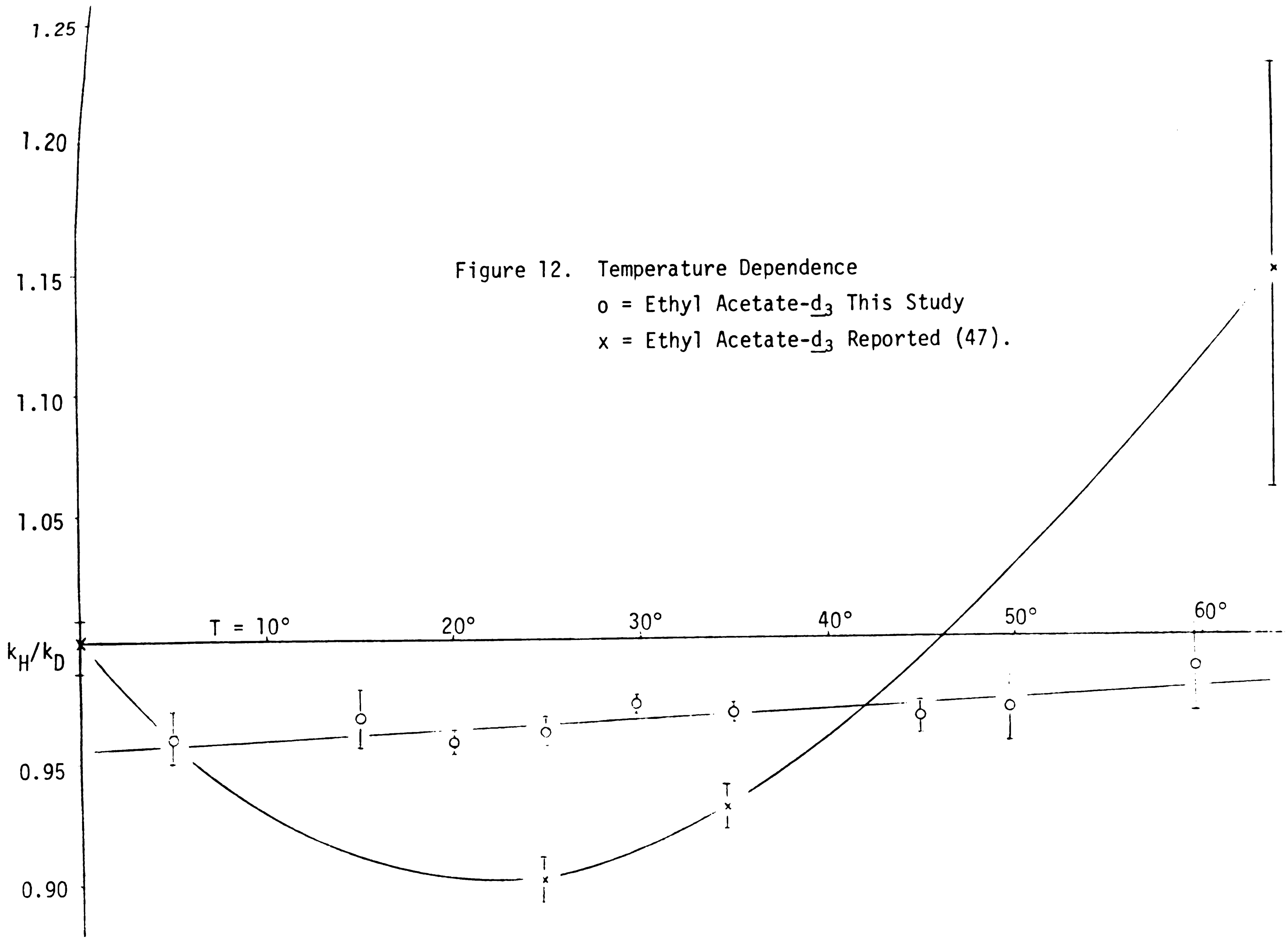

Figure 12. Temperature Dependence

o = Ethyl Acetate-$\underline{d}_3$ This Study

x = Ethyl Acetate-$\underline{d}_3$ Reported (47).

Table VI. ETHYL ACETATE

Table VI.

ETHYL ACETATE
BASE HYDROLYSIS
RATE CONSTANTS k X 10^2 l/mole-sec
AVERAGE RATES k X 10^2 l/mole-sec
RATE RATIOS

T=5.008±0.007		T=15.000±0.008		T=20.04±0.004	
H_3	D_3	H_3	D_3	H_3	D_3
2.6187	2.7205	5.4342	5.5836	7.7686	8.1382
2.6547	2.6800	5.5029	5.6596	7.7789	8.1897
2.5929	2.7149	5.4324	5.5450	7.7460	8.0991
2.5909	2.7479	5.3627	5.5515	7.7825	8.0345
2.5875	2.7274	5.4170	5.7066	7.7974	8.1132
2.6089±0.022	2.71814±0.016	5.4298±0.0320	5.6093±0.059	7.77468±0.014	8.11494±0.039
k_H/k_D=0.9589±0.010		k_H/k_D=0.968±0.012		k_H/k_D=0.958±0.0051	

Table VI. (Cont.)

Table VI. (Cont.)

T=25.006±0.003		T=29.805±0.003		T=35.000±0.003	
H_3	D_3	H_3	D_3	H_3	D_3
10.7721	11.1794	14.439	14.863	20.1467	20.5788
10.8091	11.3026	14.291	14.748	19.9483	20.5985
10.8403	11.3444	14.330	14.704	19.9087	20.5242
10.8750	11.2759	14.446	14.748	19.9945	20.7426
10.8736	11.1898	14.376±0.062	14.766±0.049	19.9908	20.6732
10.834±0.035	11.2584±0.056			19.9978±0.060	20.6235±0.068
k_H/k_D=0.9623±0.006		k_H/k_D=0.9736±0.005		k_H/k_D=0.9696±0.0044	

Table VI. (Cont.)

T=45.010±0.006		T=50.089±0.007		T=60.004±0.010	
H_3	D_3	H_3	D_3	H_3	D_3
36.8106	37.2840	43.6362	44.4621	78.8595	78.3948
36.6571	38.4677	42.8378	45.3803	79.7956	79.7382
36.6166	37.9116	43.9217	45.5099	75.6546	78.4213
36.3448	37,8377	43.7590	45.0592	77.1823	78.6845
36.6233	37.7817	44.7091	45.1029±0.34	76.3119	77.4936
36.61048±0.11	37.85654±0.27	43.7728±0.43		77.56078±1.2	78.5465±0.53
k_H/k_D=0.971±0.0076		k_H/k_D=0.9705±0.013		k_H/k_D=0.9875±0.017	

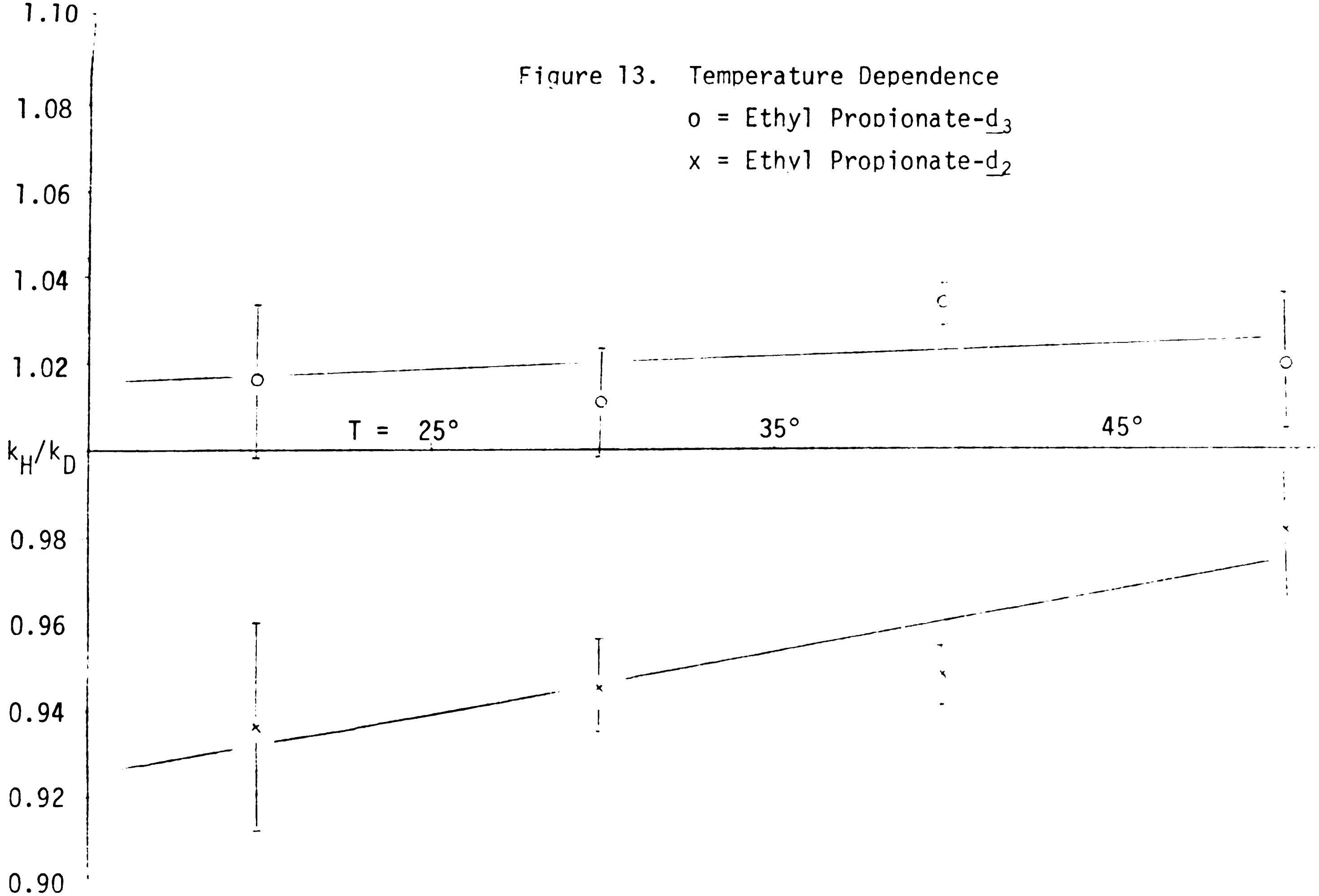

Figure 13. Temperature Dependence

o = Ethyl Propionate-$\underline{d}_3$

x = Ethyl Propionate-$\underline{d}_2$

Table VII.

ETHYL PROPIONATE
BASE HYDROLYSIS
RATE CONSTANTS k X 10^2 l/mole-sec
AVERAGE RATES k X 10^2 l/mole-sec
RATE RATIOS

T=20.025±0.006°

H_3	D_2	D_3
6.307	7.052	6.241
6.336	6.695	6.247
6.476	6.930	6.415
6.520	6.916	6.337
6.410±0.09	6.848±0.136	6.310±0.066

k_H/k_{D_2}=0.9360±0.024 k_H/k_{D_3}=1.016±0.018

T=30.000±0.01°

H_3	D_2	D_3
11.673	12.497	11.757
11.593	12.316	11.481
11.807	12.389	11.694
11.785	12.533	11.427
11.948	12.434±0.909	11.590±0.136
11.76±0.10		

k_H/k_{D_2}=0.9459±0.011 k_H/k_{D_3}=1.015±0.0145

Table VII. (Cont.)

T=40.016±0.006°

H_3	D_2	D_3
20.523	21.654	19.686
20.255	21.456	19.669
20.384	21.359	19.782
20.387±0.09	21.49±0.11	19.712±0.046

$k_H/k_{D_2}=0.94867\pm0.0064$ $k_H/k_{D_3}=1.034\pm0.005$

T=50.017±0.005°

H_3	D_2	D_3
35.666	36.646	34.360
34.667	35.659	34.280
35.798	36.398	34.456
35.154	34.146	34.365±0.06
34.146	35.712±0.8	
35.086±0.54		

$k_H/k_{D_2}=0.9825\pm0.016$ $k_H/k_{D_3}=1021\pm0.015$

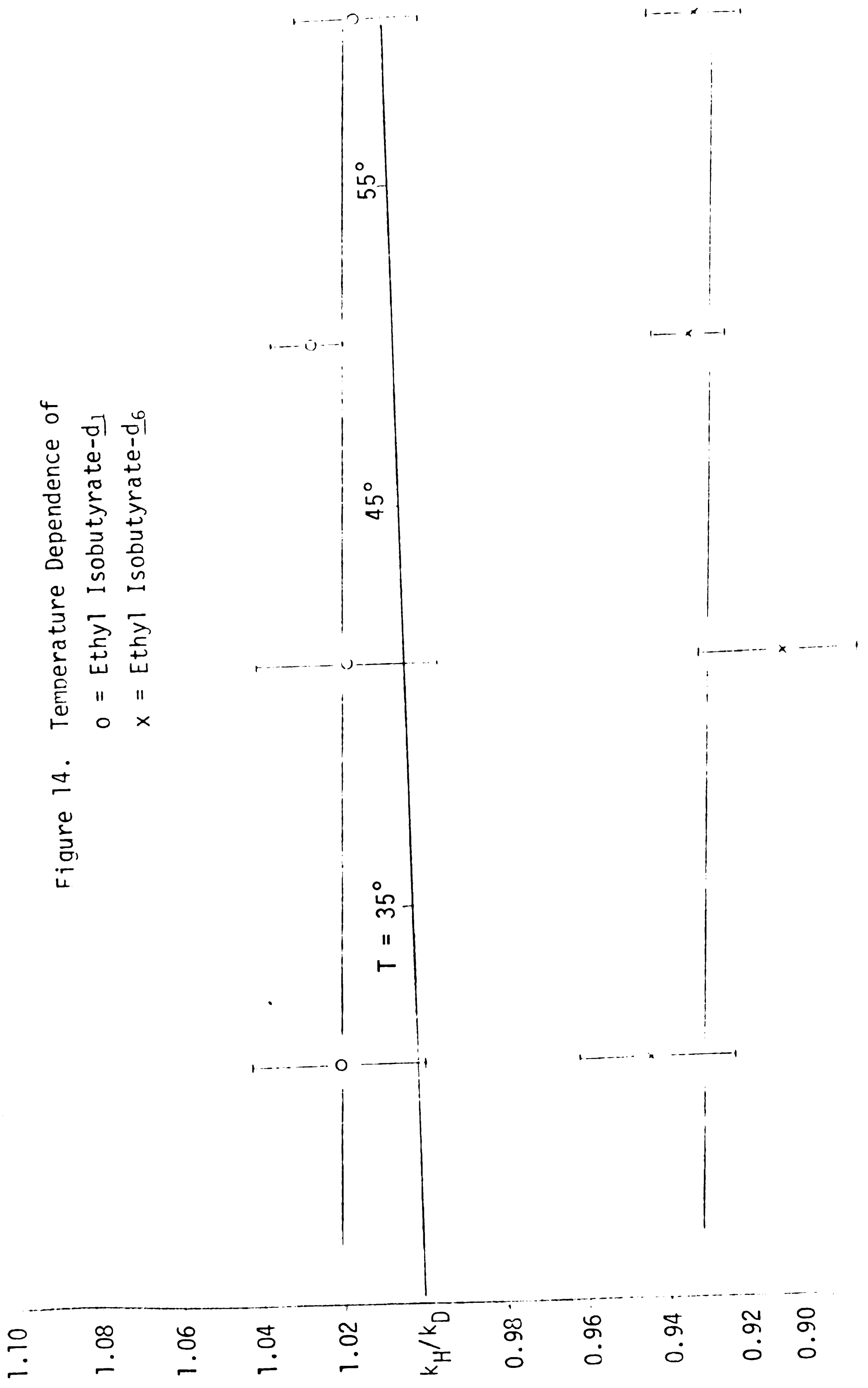

Figure 14. Temperature Dependence of

o = Ethyl Isobutyrate-d_1

x = Ethyl Isobutyrate-d_6

Table VIII.

ETHYL ISOBUTYRATE
BASE HYDROLYSIS
RATE CONSTANTS k X 10^2 l/mole-sec
AVERAGE RATES k X 10^2 l/mole-sec
RATE RATIOS

T=30.016$\pm$0.015°			T=40.032$\pm$0.003°		
H_3	D_1	D_6	H_3	D_1	D_6
3.936	3.850	4.252	6.577	6.351	6.999
4.029	4.012	4.251	6.362	6.196	7.167
4.058	3.980	4.398	6.318	6.514	7.157
4.158	4.047	4.291	6.525	6.374	7.108$\pm$0.07
4.046$\pm$0.06	3.972$\pm$0.06	4.298$\pm$0.05	6.446$\pm$0.1	6.358$\pm$0.08	

T=30.016$\pm$0.015°: $k_H/k_{D_1}=1.018\pm0.022$ $k_H/k_{D_6}=0.941\pm0.018$

T=40.032$\pm$0.003°: $k_H/k_{D_1}=1.014\pm0.022$ $k_H/k_{D_6}=0.907\pm0.020$

Table VIII. (Cont.)

T=50.017±0.01°

H_3	D_1	D_6
11.271	10.968	12.084
11.144	10.852	11.913
11.214	10.883	12.021
11.015	11.051	12.103
11.161±0.08	10.939±0.07	12.030±0.06

$k_H/k_{D_1}=1.20\pm0.010$ $k_H/k_{D_6}=0.9277\pm0.008$

T=60.012±0.015°

H_3	D_1	D_6
14.604	14.626	15.918
14.669	14.847	15.885
14.934	15.128	16.226
14.904	14.87±0.17	16.01±1.4
14.78±0.13		

$k_H/k_{D_1}=1.006\pm0.014$ $k_H/k_{D_6}=0.923\pm0.012$

Table IX. Isotope Effects at 40°[a]

	Acetate-d_3	Propionate-d_2	Propionate-d_3	Isobutyrate-d_1	Isobutyrate-d_6
k/k_{heavy}	0.972	0.960	1.02	1.016	0.926
Isotope Effect/D	0.945% (1.42%/2D)	1.98%	0.773%	1.60%	1.23%

---

[a] Based on least squares analysis.

Table X. Activation Energy Differences[a] Between Unlabeled And The Indicated Ethyl Ester

	Acetate-d_3	Propionate-d_2	Propionate-d_3	Isobutyrate-d_1	Isobutyrate-d_6
$\Delta S^*_H - \Delta S^*_D$ (cal/mole deg.)	0.1760±0.07	0.802±0.22	0.25±0.17	-0.16±0.12	-0.40±0.35
$\Delta H^*_H - \Delta H^*_D$ (cal/mole)	72.9±21.5	276.3±67	64.0±53	-59.0±38	-78±112

---

[a] Based on rate ratios in Tables VI through VIII.

Table XI. ACTIVATION PARAMETERS

Ethyl Acetate[a]

	A(10^{-7})	Ea (Kcal/mole)	ΔS* (cal/mole deg.)	ΔH* (Kcal/mole)	ΔG* (Kcal/mole)
Ethyl Acetate	1.989±0.01	11.29±0.037	-27.16±0.36	+10.684±0.11	+19.10
Ethyl Acetate-$\underline{d}_3$	1.83±0.11	11.22±0.037	-27.45±0.33	+10.580±0.099	+19.08

---

[a] Calculations based on the data in Tables VI through VIII.

Table XII. ACTIVATION PARAMETERS

Ethyl Propionate[a]

	$A(10^{-6})$	Ea (Kcal/mole)	ΔS* (cal/mole deg.)	ΔH* (Kcal/mole)	ΔG* (Kcal/mole)
Ethyl Propionate	6.44±0.89	10.750±0.085	-29.749±0.156	10.029±0.048	+19.20
Ethyl Propionate-$\underline{d}_2$	3.63±0.50	10.362±0.085	-30.550±0.145	9.753±0.045	+19.17
Ethyl Propionate-$\underline{d}_3$	4.85±0.67	10.582±0.085	-30.004±0.33	9.963±0.102	+19.21

---

[a] Calculations based on the data in Tables VI through VIII.

Table XIII. ACTIVATION PARAMETERS

Ethyl Isobutyrate[a]

	$A(10^{-5})$	Ea (Kcal/mole)	ΔS* (cal/mole deg.)	ΔH* (Kcal/mole)	ΔG* (Kcal/mole)
Ethyl Isobutyrate	1.05±0.15	8.894±0.090	-37.564±1.45	8.2908±0.46	+20.24
Ethyl Isobutyrate-$\underline{d}_1$	1.30±0.18	9.032±0.090	-37.173±1.25	8.4225±0.40	+20.25
Ethyl Isobutyrate-$\underline{d}_6$	1.27±0.18	8.962±0.090	-37.165±1.42	8.3684±0.45	+20.83

---

[a] Calculations based on the data in Tables VI through VIII.

III. Temperature Dependence

The observation of a minimum value for the rate ratio as reported by Halevi (47) is clearly inconsistent with the results of this study (Tables VI-IX). The explanation offered by Halevi for the reported minimum was based on assumed differences in energy of solvation resulting from isotopic differences in average charge distribution. These variations in solvation should be reflected in $\Delta\Delta S^*$, the difference in activation entropy between the labeled and unlabeled esters. No substantial difference has been observed (Table X).

Examination of ΔH^* and ΔS^* for the ethyl acetate, propionate, and isobutyrate hydrolyses (Table XI), and their relative contributions to the hydrolysis rates, shows that the decrease in reaction rates within this family of esters is not caused by greater ground state stabilization resulting from the inductive effects of methyl. Indeed, the activation enthalpy favors isobutyrate solvolysis. The effect comes instead from the 10 eu difference in the entropies of activation.

IV. Interpretation of Isotope Effects

A. Beta Effects

The ground state conformation of ethyl acetate (14), in which one hydrogen is eclipsing the carbonyl oxygen, has been inferred from the preferred conformation of acetaldehyde (15), which has been determined by microwave (67) and electron defraction studies (68). The observed threefold barrier to rotation about the sp^2-sp^3 carbon-carbon bond in

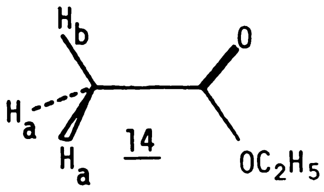

14

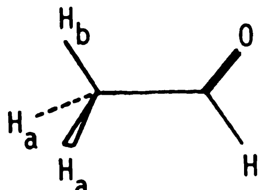

15

acetaldehyde is 1162±30 cal/mole (67). A similar conformation has been reported for acetic acid based on microwave analysis (69), but with a lower threefold barrier to rotation (483±25 cal).

The geometry of the two H_a protons is suitable for orbital overlap with the carbonyl orbital. Hyperconjugation will be more effective in the ground state than in the transition state, and will therefore lead to an inverse kinetic isotope effect (Table IX). Hyperconjugation is expected to overcome the opposing inductive effect of the H_b proton which is in the wrong orientation for hyperconjugation (8). Steric effects in this uncrowded ester are expected to be small (29).

Although the microwave analysis of propionic acid has not yet been reported (70), the conformation of ethyl propionate may be inferred from the preferred methyl eclipsing of the carbonyl (17) observed in aldehydes (71) and the conformations of several compounds containing a single halogen atom alpha to a carbonyl. The ΔH° for the equilibrium 16 ⇄ 17

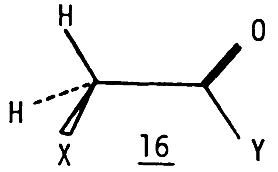

16

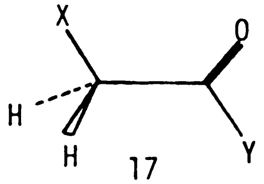

17

is -560, -500, and 0 cal/mole for ethyl fluoroacetate, chloroacetate, and bromoacetate, respectively (72); the ΔH° is -1000 cal/mole for bromoacetyl chloride and -1900 cal/mole for bromoacetyl bromide (73). For chloroacetaldehyde and bromoacetaldehyde in dimethyl sulfoxide, ΔH° is -1500 cal/mole and -700 cal/mole, respectively (74). All of these rotational isomers are best described in terms of a threefold barrier to rotation about the sp^2-sp^3 carbon-carbon bond. The percentage of ethyl propionate in the conformation with methyl eclipsing the carbonyl oxygen is expected to exceed that observed with halogen eclipsing since dipole-dipole interactions have been reduced. This assumption is supported by the observed ΔH° of -800 to -900 cal/mole (71) for propionaldehyde.

As in the case of ethyl acetate, ethyl propionate (18) has two H_a protons in a position favorable for hyperconjugation which results in an inverse isotope effect. Steric interactions, while greater than those in ethyl acetate, are not expected to be severe since both the hydroxide and the carbonyl oxygen experience only one methyl interaction in the transition state (19). Hyperconjugation is therefore the likely cause of the observed inverse isotope effect.

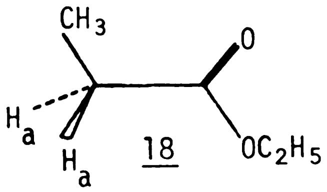

18

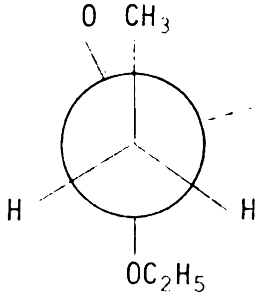

19

When one or both substituents on disubstituted acetaldehyde are methyl, methyl eclipsing of the carbonyl oxygen (20) is preferred (71).

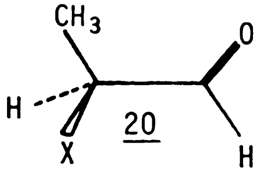

20

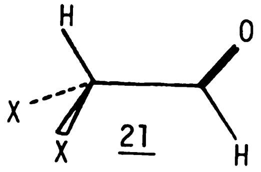

21

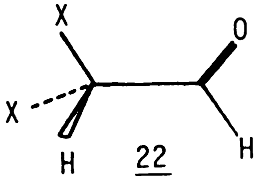

22

Dihalo substitution in aldehydes results in preferential halogen eclipsing (22) in polar solvents and hydrogen eclipsing (21) in non-polar solvents (75). Hydrogen eclipsing in dichloroacetyl chloride (76) is preferred by 200 cal/mole. All of the above are best described by a threefold barrier to rotation about the sp^2-sp^3 carbon-carbon bond, but all are also characterized by much more positive ΔH° values for

21 ⇄ 22 (75).

In contrast to mono and disubstituted aldehydes, mono and disubstituted acid halides, and monosubstituted esters, all of which exhibit threefold barriers to rotation, ethyl difluoroacetate and ethyl dichloroacetate exhibit twofold barriers to rotation with ΔH° for 23 ⇄ 24 being +25 cal/mole and 0 cal/mole, respectively (72).

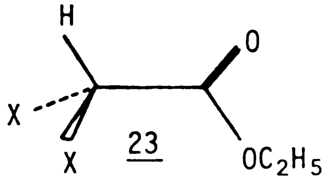

23

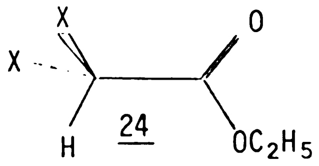

24

Although the rotation barriers of propionic acid and isobutyric acid have not yet been reported (72), the barrier in acetic acid (which is structurally similar to the ester) is substantially lower (483 cal/mole) (69) than the barrier in acetaldehyde (1162 cal/mole) (67). Acetaldehyde, monohaloacetaldehyde, and dihaloacetaldehyde all exhibit threefold barriers to rotation, while the change from ethyl monohaloacetate to ethyl dihaloacetate results in a change from a threefold barrier to a twofold barrier. It is not unreasonable to expect that other disubstituted esters, including ethyl isobutyrate, may also exhibit a twofold barrier to rotation 23 ⇄ 24.

In both conformations, 23 and 24, the orbital of the methine proton is orthogonal to the orbital of the carbonyl. Since this geometry precludes hyperconjugation, the observed normal isotope effect must be the result of inductive differences between hydrogen and deuterium.

B. Gamma Isotope Effects

In light of the above structures (18, 23, and 24), the gamma isotope effects may be readily interpreted. Carbon-carbon hyperconjugation is precluded by the orientation of the methyl in ethyl propionate. As stated earler, steric effects resulting from a single interaction are expected to be only moderate. The remaining inductive difference between hydrogen and deuterium results in the observed normal effect.

Although the inductive effect in ethyl isobutyrate-$\underline{d}_6$ should be substantial, the observation of an inverse isotope effect suggests that it is overcome by the steric effect. The presence of the second methyl group requires the carbonyl oxygen to approach one of the methyls in the more crowded transition state (Figure 10). This conformation also results

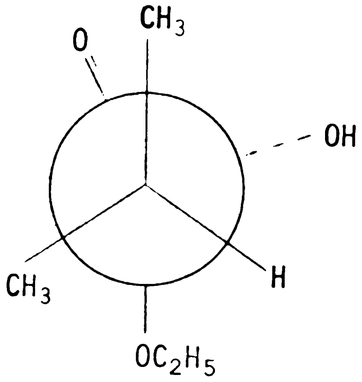

Figure 10. Steric Interactions in Ethyl Isobutyrate Hydrolysis.

in interaction between one of the methyls and the attacking hydroxide. Carbon-carbon hyperconjugation may also be contributing to the large inverse isotope effect.

V. Solvation Effects

Although the anomalous isotope effects of ethyl isobutyrate have been explained in terms of a twofold barrier to rotation, the results are not necessarily inconsistent with a threefold barrier. It has been noted that the activation entropy is substantially larger for ethyl isobutyrate than for ethyl propionate or ethyl acetate. This difference is undoubtedly due to steric inhibition of solvation in the ground state of ethyl isobutyrate resulting from interactions with methyl. A consequence of this is an increased demand for solvation on the side away from the methyl group (25). Interference between the alcohol moiety and solvent will tend to move the alcohol away from its preferred planer conformation into a position nearer the methyl. The resulting torsional effect on the sp^2-sp^3 carbon-carbon bond, combined with torsional effects resulting from interaction between the non-bonded electron pairs of the alcohol oxygen and the methyl, increase the dihedral angle between the carbon-hydrogen (deuterium) bond and the π orbital with which it is to hyperconjugate. This angle, without consideration of

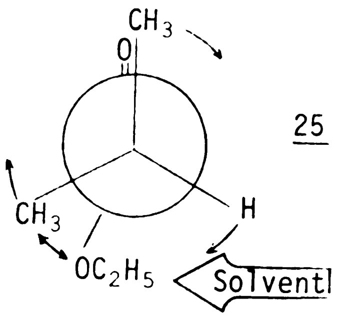

25

torsional effects, is 30°. A 30° angle still allows an overlap with greater than 85% of the effectiveness of parallel orbitals, but it is to the point at which orbital overlap begins to deteriorate rapidly as dictated by the cosine relationship $\beta = \beta_o \cos \theta$ (77). Torsional effects, if indeed they exist, could destroy the orbital overlap which would also eliminate hyperconjugation. Steric effects from this position are expected to be slight, and the remaining indicative effect would lead to the observed normal effect.

A small contribution to the rate determining step by the process involving ethoxide expulsion would tend to counteract the isotope effects involved in hydroxide attack, the two steps being essentially the reverse of each other. Since a more crowded transition state would lead to increases in both activation barriers,as well as the instability of the tetrahedral intermediate, it is not clear what effect crowding should have on the isotope effects.

VI. Conclusion

In conclusion, the inverse β isotope effects observed with ethyl acetate and ethyl propionate have been explained by hyperconjugation. The γ normal isotope effect in ethyl propionate is believed to be the result of inductive effects while the γ inverse effect observed in ethyl isobutyrate is very likely steric in origin in this crowded system, with a possible enhancement by carbon-carbon hyperconjugation. The observation of a normal β isotope effect with ethyl isobutyrate is considered to be evidence for a change from a threefold barrier to rotation to a twofold barrier. Torsional effects on a threefold barrier **have also** been considered.

The objective of this study was to confirm or deny the unprecedented temperature dependence of the isotope effect reported by Halevi in the alkaline hydrolysis of ethyl acetate-$\underline{d}_3$ and to extend the temperature study to include the isotope effects of ethyl propionate and ethyl isobutyrate. Although the objectives have been fulfilled through the implementation of two rapid and accurate analytical techniques, and explanations for the observed isotope effects have been offered, the implication of the β isotope effect of ethyl isobutyrate-$\underline{d}_1$ should be considered evidence for rather than proof of a twofold barrier to rotation in ethyl isobutyrate.

EXPERIMENTAL

I. Ester Preparation

A. Ethyl Acetate-$\underline{d}_3$ and Unlabeled Ethyl Acetate

Ethyl acetate-$\underline{d}_3$ (99%-D) was purchased from Merck Sharp & Dohme Lot No. C-188. Mass spectral, nmr, and glc on carbowax analyses confirmed its chemical and isotopic purity. "Baker Analyzed" reagent ethyl acetate was distilled and used without further purification.

B. Ethyl Propionate-2,2-$\underline{d}_2$; -3,3,3-$\underline{d}_3$; and Unlabeled Ethyl Propionate

All ethyl propionate were prepared by the method of Nolin and Leitch (78). Five and one half gram samples (0.074 moles) of distilled Fisher certified propionic acid, Merck Sharp & Dohme propionic-2,2-$\underline{d}_2$ acid-$\underline{d}$ (98%-D) and propionic-3,3,3-$\underline{d}_3$ acid (98%-D) were cooled, diluted tenfold with water, and neutralized with a cold ten per cent aqueous ammonia to a pH between 7.5 and 8.5. A twenty molar per cent excess of silver nitrate solution was added and the resulting white silver salt filtered, washed first with water and then ethanol, and finally dried over night in a vacuum oven. The yield was generally 98%.

To the dry silver salt was added an equal molar amount of distilled ethyl iodide and, with exclusion of water, the two were allowed to reflux over night yielding 86% of the desired ester.

Gas chromatographic analysis of the crude distalate indicated an impurity level of approximately 0.4%. Washing with water, extraction with ether, removal of ether under reduced pressure, and finally isolation by preparative glc on an 80 inch, 20% carbowax on chromasorb W column afforded pure ethyl propionates. Mass spectral, glc on carbowax and FFAP, and nmr analysis confirmed the chemical and isotopic purity of the esters.

All ethyl propionates exhibited the characteristic nmr ethyl quartet and triplet at 6.26 and 9.13 τ. The unlabeled ethyl propionate spectra contained a second methyl triplet at 9.28 τ, overlapping the ethyl triplet, and a methylene quartet at 8.10 τ.

Labeled ethyl propionates exhibited the same spectra except that ethyl propionate-2,2-$\underline{d}_2$ lacked the methylene triplet,and its second methyl degenerated into a multiplet at 9.27 τ. Ethyl propionate-3,3,3-$\underline{d}_3$ exhibited the methylene at 8.13 τ as a multiplet and lacked the second methyl peak.

C. Ethyl 2-Methylpropanoate; Labeled and Unlabeled

Ethyl 2-methyl-$\underline{d}_3$ -propanoate-3,3,3-$\underline{d}_3$, ethyl 2-methylpropanoate-2-$\underline{d}_2$,and unlabeled ethyl 2-methylpropanoate were prepared from their parent acids, purified, and analyzed by the same procedure as the ethyl propionates. Sym-isobutyric-$\underline{d}_6$ acid (99.5%-D) was prepared by Adan Effio by the following process:

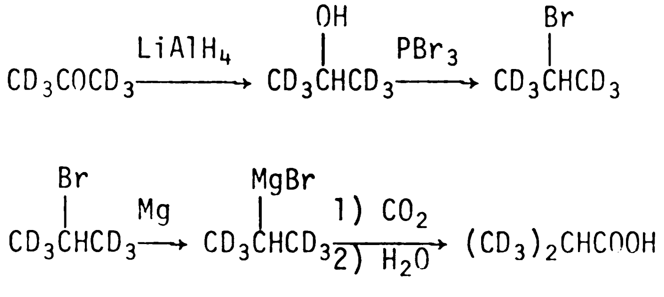

$$\mathrm{CD_3COCD_3} \xrightarrow{\mathrm{LiAlH_4}} \mathrm{CD_3\overset{OH}{C}HCD_3} \xrightarrow{\mathrm{PBr_3}} \mathrm{CD_3\overset{Br}{C}HCD_3}$$

$$\mathrm{CD_3\overset{Br}{C}HCD_3} \xrightarrow{\mathrm{Mg}} \mathrm{CD_3\overset{MgBr}{C}HCD_3} \xrightarrow[2)\ \mathrm{H_2O}]{1)\ \mathrm{CO_2}} \mathrm{(CD_3)_2CHCOOH}$$

Isobutyric-α-d acid was prepared by pyrolysing dimethylmalonic acid-d_2 at a temperature of 180° for 12 hours. The labeled dimethylmalonic acid was the product of five exchanges of the unlabeled dimethylmalonic acid (Aldrich Chemical Co.). with D_2O (99%-D)

In addition to the ethyl quartet and triplet at 6.22 and 9.06 τ present in the nmr spectra of all ethyl isobutyrates, the unlabeled ester spectrum contained a two methyl double at 9.15 τ and a broad methine multiplet at 7.86 τ.

The ethyl isobutyrate-d_6 spectrum lacked the two methyl doublet, and the multiplet had degenerated into a broad singlet at 7.81 τ. The spectrum of ethyl isobutyrate-α-d lacked the multiplet, and the two methyl doublet reduced to a broad singlet at 9.15 τ.

II. Procedure

A. Base Preparation

Carbonate free base was prepared by the method of Albert and Serjeant (79). Fourteen grams of reagent grade potassium hydroxide was dissolved in 1.5 liters of distilled water. A solution containing three grams of barium hydroxide was added, the flask inverted, and the barium carbonate precipitate was allowed to settle overnight.

Solution was drawn out of the flask through a tube protruding beyond the precipitate and into a Dowex 50W-X8 cation exchange column saturated with potassium ion in order to remove the barium ion present. Dilution of 100 ml of this 0.16 N solution with three liters of freshly boiled conductance water under nitrogen atmosphere afforded carbonate free base of the approximately 0.005 normality desired.

Base concentration was determined by titration against seven samples of oven-dried Fisher Primary Standard potassium hydrogen phthalate weighed on a five decimal place Mettler balance using Bromo Thymol Blue indicator.

B. pH Monitoring

An Instrumentation Laboratory model 245 scale expanding pH meter was used to continuously monitor the pH. The electrode used was an Instrumentation Laboratory model 14063 high alkaline combination electrode. When not in use, the electrode was stored in dilute hydrochloric acid at the next temperature to be investigated.

The output of the pH meter was recorded on a Sargent model SL recorder. All determinations were made in the scale expanded mode. One pH unit represented a 10-inch deflection on both the meter and recorder. No decernable variation between the meter and recorder appeared over this range.

The chart speed of the recorder proved to be sufficiently accurate to provide the time base for the readings.

C. Constant Temperature Bath

Temperature was maintained during the hydrolyses by a 25-liter constant temperature bath. The bath was insulated on its sides and bottom with one inch of styrofoam supported by 5/8 inch plywood. The top of the bath was covered with a tight-fitting 1/4 inch reinforced plexiglas cover.

From the top were suspended a Troemner immersible magnetic stirrer, a Precision Scientific Co. number 62541 thermoregulator (±0.005F°), and a Teel number 1p622 circulating pump. A sample cell 2.50 inches long blown from 19mm glass tubing was inserted through a tight-fitting hole and came to rest centered on the stirrer with its top flush with the top of the cover. Two additional holes were provided in the top through which additional sample cells could be suspended to allow complete thermal pre-equalibration.

D. Temperature Control

The bath was cooled or heated as required. Circulation of tap water from a constant pressure device through three feet of internal 1/4 inch copper tubing provided adequate cooling for temperatures down to 15°. A temperature of 5° was obtained by pumping ethylene glycol at 0° from a second bath through the cooling coil.

In both cases, and at higher temperatures, the temperature was controlled by intermittent heating with a 200-watt heating coil, activated by the thermal controller's switching of a relay switch. The amount of heating was limited by a triac clipping circuit until the "off time" and "on time" were equal. Both the relay and clipping unit were built by the author. For temperatures above 65°, an additional continuous heater capable of supplying up to 100 watts was added.

E. Quartz Thermometer

Bath temperatures were measured with a Hewlett-Packard model 2801A Digital Quartz thermometer. Zero point calibration of probes was performed in a three liter ice water Dewar flask mounted on a low speed mechanical shaker. Bath temperature variation was found to be less than ±0.007° over the range +15 to +65°.

F. Rate Determinations

At the beginning of each set of measurements, the electrode was rinsed with distilled water, placed in Instrumentation Laboratory number 31060 pH 6.84 buffer (the isoelectric point of the electrode) and the meter balance adjusted. After two more washings, electorde was placed in a Matheson, Coleman & Bell pH 10.00 buffer and the appropriate correction made with the pH/MV slope control.

Following two additional washings, 3.88 ml of the standardized potassium hydroxide was dispensed into a sample cell from a 5 ml burette and transferred under nitrogen atmosphere to the bath.

All washings, buffers, and base samples were thermally pre-equalibrated in order to avoid electrode hysteresis upon cooling (79).

Six minutes was allowed to elapse while the electrode adjusted to the base. At that time the balance of the pH meter was adjusted to a scale expanded value of 10.95. Fifteen micro liters of ester was injected through septum into the stirred base as the recorder passed a convenient measuring point. Recording was continued until a pH of 10.00 was reached, at which time the electrode was washed, new base added, and the process repeated.

The first two runs were always discarded to avoid inconsistencies resulting from incomplete electrode conditioning. Subsequent runs were alternated between unlabeled and the one or two labeled esters.

G. Treatment of Data

Times read from the recording were taken at 0.05 pH unit intervals from pH 10.90 to 10.05. These values, corresponding to 2.9 half-lines of base, were analyzed by the second order rate program SEC R (Figure 11).

```
 SECR      FORTRAN EXTENDED VERSION 2.0    (210)     08/13/70

      PROGRAM SEC R (INPUT,OUTPUT,TAPE2=INPUT,TAPE3=OUTPUT)
      DIMENSION T(100),H(100),Y(100),TITLE (40),PH(100),X(100),
     1 DELTA(100),DEL T(100),PHOES(100)
    1 READ (2,101)  TITLE
  101 FORMAT(     40A2)
    2 READ (2,102)  N,EZERO,OH IN,EX,PHOFF,TOFF
  102 FORMAT (I3,5F10.6)
      WC = 10.0**(-EX)
      IF (N-1) 500,1000,3
    3 DO 4 I=1,N
      READ (2,103)  PH(I),T(I)
  103 FORMAT (F9.5,F10.5)
      PHOES(I)=PH(I)
      PH(I)=PH(I)+PHOFF
      T(I)=T(I)+TOFF
      X(I) = T(I)*60.00
      H(I)=EXP(-2.30258*PH(I))
    4 Y(I)=(1.0/(OH IN -EZERO))*(ALOG(EZERO/(EZERO+WC/H(I)-OH IN))
     1    -ALOG(H(I)*OH IN /WC))
C     COMPUTE INTERVALS BETWEEN TIMES
      NN=N-1
      DO 8 I=1,NN
      DEL T(I)=T(I+1)-T(I)
    8 DEL T(N)=0
      GO TO 11
C     OMIT RATES AND BECOME LEAST SQUARES
  500 READ(2,116)N
  116 FORMAT(I2)
      IF (N) 1000,1000, 10
   10 DO 9 I=1,N
      READ(2,103)Y(I),T(I)
      DEL T(I)=0
      X(I)=T(I)
      PHOES(I) = 0
      PH(I)=0
    9 H(I)=0
C     COMPUTE SUMS
   11 SIGX = 0
      SIGX2 = 0
      SIGY = 0
      SIGY2 = 0
      SIGXY = 0
      DO 5 I=1,N
      SIGX = SIGX + X(I)
      SIGX2 = SIGX2 + (X(I)**2)
      SIGY = SIGY + Y(I)
      SIGY2 = SIGY2 + (Y(I)**2)
    5 SIGXY = SIGXY + (X(I)*Y(I))
C     COMPUTE A,B ETC.
      Q = N
      D = (Q*SIGX2) - (SIGX**2)
      A = ((Q*SIGXY) - (SIGX*SIGY)) / D
      B = ((SIGX2*SIGY) - (SIGX*SIGXY)) / D
```

Figure 11. Second Order Rate Program 'Sec R'

```
SECR       FORTRAN EXTENDED VERSION 2.0    (210)     08/13/70

      SY2 = 0
      DO 6 I=1,N
    6 SY2 = SY2 + ((Y(I) - B - (A*X(I)))**2)
      SY2 = SY2 / (Q-2.0)
      SY = SQRT (SY2)
      SA2 = (Q*SY2) / D
      SA = SQRT (SA2)
      SB2 = (SY2*SIGX2) / D
      SB = SQRT (SB2)
      E = (Q*SIGY2) - (SIGY**2)
      F = SQRT (D*E)
      CORR = ((Q*SIGXY) - (SIGX*SIGY)) / F
      IF(CORR) 21,22,22
   21 CORR = -CORR
   22 CONTINUE
      DO 23 I=1,N
   23 DELTA(I) = Y(I)-B-(A*X(I))
C       OUTPUT
      WRITE(3,104) TITLE
  104 FORMAT(1H1,40A2)
      WRITE (3,105)
  105 FORMAT(2H      ///////)
      WRITE (3,106)
  106 FORMAT (7X,5HDEL T,6X,9HT,MINUTES,6X5HPHUSE,3X,2HPH,4X,
     119HH-ION CONCENTRATION,10X,4HY(I),10X,8HDELTA(I))
      WRITE (3,107)
  107 FORMAT (/)
      DO 7 I = 1,N
    7 WRITE(3,108)DEL T(I),T(I),PHUES(I), PH(I),H(I), Y(I), DELTA(I)
  108 FORMAT (8X, F4.2, 8X, F6.2, 5X, F5.2, 2X, F7.4,      E15.5,
     1 4X, E17.5, 1X, E15.5)
      WRITE (3,115)
  115 FORMAT (//////)
      WRITE (3,109)    A, SA
  109 FORMAT (8H SLOPE =    E14.6///
     1  21H STD. DEV. OF SLOPE =          E14.6  /////    )
      WRITE (3,110)   B,SB
  110 FORMAT (12H INTERCEPT =             E14.6     ///
     1    25HSTD. DEV. OF INTERCEPT =          E14.6  /////  )
      WRITE (3,111)   SY, CORR
  111 FORMAT (19H STD. DEV. OF FIT =       E14.6    /////
     1    26H CORRELATION COEFFICIENT =       F9.5  )
      WRITE (3,112)   EZERO
  112 FORMAT(/////30H INITIAL ESTER CONCENTRATION = ,F15.10)
      WRITE (3,113) OH IN
  113 FORMAT(//30H INITIAL BASE CONCENTRATION = ,F15.10)
      WRITE (3,114)   WC
  114 FORMAT(//5H KW =  F15.5)
      GO TO 1
 1000 CALL EXIT
      END
```

Figure 11 (Cont.)

This program was written by the author with the assistance of Professor Schiavelli. The program first corrected all the pH values from the starting point of 10.95 to the calculated value appropriate to the known base concentration at the temperature studied.

Second order rate constants were then obtained by a least squares solution of the special integrated second order rate equation:

```
KT = (1.0/(OHZERO-EZERO))*(ALOG(EZERO/(EZERO          (I)
     +WC/H(I)-OHZERO))-ALOG(H(I)*OHZERO/WC))
```

OHZERO = initial base concentration
EZERO = initial ester concentration
WC = ion product of water at bath temperature
H(I) = hydrogen ion concentration at time T

which was derived from the standard integrated second order rate equation:

$$kt = \frac{1}{b-ra}\left(\ln\left(\frac{a}{a-x}\right) - \ln\frac{[(b/r)\ \ ]}{[(b/r)-x]}\right)$$

a = initial concentration of A
b = initial concentration of B
r = stichometric factor
x = concentration change in A at time t

Lines with negligible curvature resulting in correlation coefficients greater than 0.999 were consistently obtained. The rates reported are averages of at least three and usually four independent rate determinations. The uncertainty indicated is the average deviation, σ.

$$\sigma = \frac{1}{n}\ {}_i\ \Sigma\ (x_i - \bar{x}_i)$$

x_i = observed rate

$\bar{x}_i$ = mean

Rate ratios, k_H/k_D, are the ratios of the resulting means. The uncertainty indicated is the standard deviation obtained from the relationship.

$$\sigma_{k_H/k_D} = \bar{k}_H/\bar{k}_D\sqrt{(\sigma_H/k_H)^2 + (\sigma_D/k_D)^2}$$

The average rate constants at different temperatures were used to determine the thermodynamic activation parameters ΔS^* and ΔH^* from the equation.

$$\log\ (\bar{k}/T) = \frac{-\Delta H^*}{2.30258RT} + \frac{\Delta S^*}{2.30358R} + \log\ (k/h)$$

$\bar{k}$ = average rate constant
T = absolute temperature
R = gas constant
k = Boltzmann's constant
h = Plank's constant

Activation paramerers were calculated by two computer programs: ACTENG and ACTIV. The former, written by Professor DeTar, utilizes a weighted iterative least squares solution while the latter, by Professor Sonnicksen, utilizes a single least squares solution of the relationship log ($\bar{k}$/T) versus 1/T.

Enthalpy and entropy of activation differences ($\Delta\Delta H^*$ and $\Delta\Delta S^*$) were evaluated (80) by a least squares solution of the relationship ln k_H/k_D versus 1/T in the equation:

$$\ln (\bar{k}_H/\bar{k}_D) = \frac{-\Delta\Delta H^*}{RT} + \frac{\Delta\Delta S^*}{R}$$

by the program HAND, written by Professor Sonnichsen.

BIBLIOGRAPHY

(1) M. Wolfsberg and M. J. Stern, *Pure Appl. Chem.*, **8**, 325 (1964).

(2) E. S. Lewis and C. E. Boozer, *J. Am. Chem. Soc.*, **74**, 6306, 1952).

(3) A. Streitweiser, Jr., R. H. Jagow, R. C. Fahey, and S. Suzuki, *ibid.*, **80**, 2326 (1958).

(4) R. E. Weston, Jr., *Science*, **158**, 332 (1967).

(5) M. Wolfsberg and M. J. Stern, *Pure Appl. Chem.*, **8**, 225 (1964).

(6) M. J. Stern and M. Wolfsberg, *J. Chem. Phys.*, **45**, 4105 (1966).

(7) E. A. Halevi, "Secondary Isotope Effects" in "Progress in Physical Organic Chemistry," ed. Cohen, Streitwieser, and Taft, Vol. 1, Interscience, 1963, (a) p 109, (b) p 152, (c) p 153.

(8) V. J. Shiner, Jr., *J. Am. Chem. Soc.*, **82**, 2655 (1960).

(9) V. J. Shiner, *ibid.*, **86**, 2643 (1964).

(10) Indiana University Conference on Hyperconjugation, *Tetrahedron*, **5**, 105-274 (1959).

(11) W. M. Schubert, J. M. Craven, R. G. Minton, and R. B. Murphy, *ibid.*, **5**, 105-274 (1959).

(12) E. Berliner, *ibid.*, **5**, 202 (1959).

(13) R. W. Taft and I. C. Lewis, *ibid.*, **5**, 210 (1959).

(14) H. C. Brown, J. D. Brady, M. Grayson, and W. H. Bonner, *J. Am. Chem. Soc.*, **79**, 1897 (1957).

(15) H. C. Brown, B. A. Bolto, and F. R. Jensen, *J. Org. Chem.*, **23**, 414 (1958).

(16) S. Ehrenson, *J. Am. Chem. Soc.*, **86**, 847 (1964).

(17) F. R. Jensen, B. E. Smart, *ibid.*, **91**, 5686 (1959).

(18) a) E. A. Halevi, M. Nussim, and A. Ron, *J. Chem. Soc.*, 866 (1963); b) E. A. Halevi, *Tetrahedron*, **1**, 174 (1967).

(19) E. A. Halevi, E. N. Haran, and B. Ravid, *Chemical Physics Letters*, **1**, 475 (1967).

(20) G. V. Tiers, *J. Chem. Phys*., **29**, 963 (1958).

(21) G. V. Tiers, *J. Am. Chem. Soc*., **79**, 5585 (1957).

(22) H. C. Brown, M. E. Azzaro, J. G. Koelling, and G. J. McDonald, *ibid*., **88**, 2520 (1966).

(23) a) K. Mislow, M. A. W. Glass, H. B. Hopps, E. Simon, and G. H. Wahl, Jr., *ibid*., **86**, 1710 (1964).

(24) K. Mislow, R. Graeve, A. J. Gordon, and G. H. Wahl, Jr., *ibid*., **86**, 1733 (1964).

(25) L. Melander, *ibid*., **86**, 295 (1964).

(26) R. E. Carter and E. Junggren, *Acta Chem. Scand*., **22**, 503 (1968).

(27) L. S. Bartell, *J. Chem. Educ*., **45**, 754 (1968).

(28) L. S. Bartell and R. A. Bonhan, *J. Chem. Phys*., **32**, 824 (1960).

(29) G. C. Sonnichsen, Ph.D. Thesis, Michigan State University, East Lansing, MI., 1967.

(30) L. S. Bartell, *J. Am. Chem. Soc*., **83**, 3567 (1961).

(31) V. J. Shiner, Jr., and J. O. Stoffer, *ibid*., **92**, 3192 (1970).

(32) V. J. Shiner, Jr., W. E. Buddenbaum, B. L. Murr, and G. Lamaty, *ibid*., **90**, 418 (1968).

(33) V. J. Shiner, Jr., W. Dowd, R. D. Fisher, S. R. Hartshorn, M. A. Kessick. L. Milakofsky, and M. W. Rapp, *ibid*., **91**, 4838 (1969).

(34) V. J. Shiner, Jr., M. W. Rapp, E. A. Halevi, and M. Wolfsberg, *ibid*., **90**, 7171 (1968).

(35) V. J. Shiner, Jr., W. E. Buddenbaum, B. L. Murr, and G. Lamaty, *ibid*., **90**, 418 (1968).

(36) G. E. Jackson and K. T. Leffek, *Can. J. Chem*. **47**, 1537 (1969).

(37) S. Seltzer and A. Zavitsas, *ibid*., **45**, 2023 (1967).

(38) G. S. Hammond, *J. Am. Chem. Soc.*, **77**, 334 (1955).

(39) L. Hakka, A. Queen, and R. E. Robertson, *J. Am. Chem. Soc.*, **87**, 161 (1965).

(40) K. T. Leffek, R. E. Robertson, and S. E. Sugamori, *Can. J. Chem.*, **39**, 1989 (1961).

(41) K. T. Leffek, J. A. Llewellyn and R. E. Robertson, *J. Am. Chem. Soc.*, **82**, 6315 (1960).

(42). J. D. Swalen and C. C. Costain, *J. Chem. Phys.*, **31**, 1562 (1959)

(43) R. E. Robertson, *Can J. Chem.*, **42**, 1707 (1964).

(44) R. E. Robertson and S. E. Sugamori, *J. Am. Chem. Soc.*, **91**, 7254 (1969).

(45) M. J. Blandamer, H. S. Golinkin, and R. E. Robertson, *ibid.*, **91**, 2678 (1969).

(46) G. J. Karabatsos and C. G. Papioannou, *Tetrahedron Lett.*, **22**, 2629 (1968).

(47) E. A. Halevi and Z. Margolin, *Proc. Chem. Soc.*, 174 (1964).

(48) M. L. Bender and M. S. Feng, *J. Am. Chem. Soc.*, **82**, 6318 (1960)

(49) A. Streitwiser, Jr., C. S. Wilkins, and E. Kiehlmann, *ibid.*, **90**, 1598 (1968).

(50) J. B. Hyne and R. E. Robertson, *Can. J. Chem.*, **33**, 1536 (1955).

(51) E. C. Ashly, R. B. Duke, and H. M. Neuman, *J. Am. Chem. Soc.*, **89**, 1964 (1967).

(52) T. Holm, *Acta. Chem. Scand.*, **23**, 579 (1969).

(53) R. Warder, *Chem. Ber.*, **14**, 1361 (1881).

(54) M. L. Bender, *J. Am. Chem. Soc.*, **73**, 1626 (1951).

(55) A. Moffat and H. Hunt, *ibid.*, **81**, 2082 (1959).

(56) S. L. Johnson, "Advances in Physical Chemistry," V. Gold, Ed., Academic Press, Inc., London, 1967.

(57) E. S. Gould, "Mechanism and Structure in Organic Chemistry," Holt, Rinehart, and Winston, New York, N. Y., 1959.

(58) J. R. Dyer, "Applications of Absorption Spectroscopy of Organic Compounds," Prentice-Hall, Inc., Englewood Cliffs, NJ, 1965.

(59) G. A. Olah and P. R. Schleyer, "Carbonium Ions. Volume I. General Aspects and Methods of Investigation," John Wiley and Sons, Inc., New York, N. Y. (1968).

(60) B. L. Murr, Jr., and V. J. Shiner, Jr., *J. Am. Chem. Soc.*, **84**, 4672 (1962).

(61) J. D. Morrison and R. W. Ridgway, *ibid.*, **91**, 4601 (1969).

(62) C. G. Enke, Michigan State University, personal communication, 1970.

(63) R. A. Peters and E. Walker, *Biochem. J.*, **17**, 260 (1923).

(64) B. N. Heudy, W. A. Redmond, and R. E. Robertson, *Can. J. Chem.*, **45**, 2071 (1967).

(65) M. R. Wright, *J. Chem. Soc.*, *Sect. B*, 545 (1968).

(66) I. Klotz, "Chemical Thermodynamics," W. A. Benjamin, Inc., New York, N. Y., 1964, p 417.

(67) R. W. Kilb, C. C. Lin, and E. B. Wilson, Jr., *J. Chem. Phys.*, **26**, 1695 (1957).

(68) R. Schwendeman, Michigan State University, personal communication, 1970.

(69) W. J. Taber, *J. Chem. Phys.*, **27**, 974 (1957).

(70) O. L. Stiefvater, University of Birmingham, England, personal communication, 1970.

(71) N. C. T. Hsi, Ph.D. Thesis, Michigan State University, East Lansing, MI., 1966.

(72) T. L. Brown, *Spectrochim. Acta*, **18**, 1615 (1962).

(73) S. Mizushima, T. Schimanouchi, T. Miyazawa, I. Ichishima, K. Kuratani, I. Nakagawa, and N. Shido, *J. Chem. Phys.*, **21**, 815 (1953).

(74) G. J. Karabatsos and D. J. Fenoglio, *J. Am. Chem. Soc.*, **91**, 1124 (1969).

(75) G. J. Karabatsos, D. J. Fenoglio, and S. S. Lande, *ibid.*, **91**, 3572 (1969).

(76) A. Miyake, I. Nakagawa, I. Ichishima, T. Schimanouchi, and S. Mizushima, *Spectrochim. Acta*, **13**, 161 (1958).

(77) A Streitwiser, Jr., "Molecular Orbital Theory for Organic Chemists," John Wiley and Sons, Inc., New York, N. Y., 1961.

(78) B. Nolin and L. C. Leitch, Can. J. Chem., **31**, 153 and 1257 (1953).

(79) A. Albert and E. P. Serjeant, "Ionization Constants of Acids and Bases," John Wiley & Sons, Inc., New York, N. Y., 1962, p 23.

(80) K. B. Wiberg, "Physical Organic Chemistry," John Wiley & Sons, Inc., New York, N. Y., 1964.